

1 **Editor Comments**

2  
3 Many thanks for answering the comments raised by the different  
4 reviewers. This manuscript should be accepted but it would be nice to  
5 address the few points raised by the reviewer 3 on the coherency  
6 between the SP19 and WP2014 chronologies (and potential  
7 implications for a future WAIS chronology) in a revised manuscript.  
8 Thanks again for your efforts.

9  
10 **Thank you very much for your positive assessment of our article. Below are our**  
11 **responses to the reviewer comments as well as a revised manuscript. As you**  
12 **requested, we have addressed the points raised by reviewer 3. This includes the**  
13 **addition of a new figure showing the coherency between SP19 and WD2014 (Fig.**  
14 **S5). Our revisions also include clarification about the implications for the existing**  
15 **WD2014 timescale (lines 798-801 in this document).**

16  
17 **Review #1**

18  
19 **Thank you very much for the very useful and positive comments. We greatly**  
20 **appreciate your input. Below are our line-by-line responses to your review.**

21  
22 Winski et al. present a first chronology, named SP19, for the South Pole Ice Core  
23 (SPICECore), back to 54,302 yr BP. This chronology is based on a combination of  
24 251 volcanic matching to the WAIS Divide ice core and annual layer counting (back to  
25 11,341 yr BP for the latter). More precisely, the SP19 chronology is strictly tied to the  
26 WD2014 chronology at the depth of the volcanic matches, and then layer counting is  
27 used to interpolate in-between. Before 11,341 yr BP, a spline interpolation method is  
28 used instead of annual layer counting. The layer counting is based on CFA measurements  
29 of magnesium, sodium, sulfate, chloride and dust. It has been performed by  
30 4 different operators and reconciliation is found a posteriori when there is a discrepancy.  
31 A comparison is also made with visual stratigraphy but chemical stratigraphy is  
32 preferred because it is found to be more accurate.

33  
34 It is argued that the WD2014 is used because it is more precise (annual layer thickness  
35 is larger at WD) and to have a WD2014 compatible time scale. The relative uncertainty  
36 to WD2014 is small during the Holocene, generally less than 18 yr and always less  
37 than 25 yr. For older parts, the relative uncertainty to WD2014 is less than 124 yr.  
38 The accumulation rate which is found in the SPICEcore is found to be mainly due to  
39 the upstream spatial pattern of accumulation along the flow line. The accumulation  
40 reconstruction is also compatible with nitrate concentration, nitrate amplitude of seasonal  
41 variations and N-15 of N2 in air bubbles (through a dynamical Herron-Langway  
42 firm model for the latter). It is therefore argued that the SPICEcore is a good candidate  
43 to test the influence of surface accumulation rate on the Lock-In Depth.

44  
45 This article is very well written and its content is consistent. I therefore recommend to  
46 accept it.

47 **Thank you.**

48  
49 I only have a few technical corrections.  
50 - l. 385: suppress "accumulation rate" since it is actually not plotted on this figure.  
51 **Done.**  
52  
53 l. 489, l. 531 and l. 535: double space after dot.  
54 **Fixed.**  
55

## 56 **Review #2**

57  
58 **Thank you very much for the very useful and positive comments. We greatly**  
59 **appreciate your input. Below are our line-by-line responses to your review.**  
60

61 In the paper “The SP19 Chronology for the South Pole Ice Core - Part 1: Volcanic  
62 matching and annual-layer counting” by D. A. Winsky and co-authors a new timescale  
63 (called SP19) for the SPICEcore is presented. This new time scale was partly achieved  
64 by annual layer counting but the main guide to build the age scale is a robust volcanic  
65 match coming from a comparison with WAIS Divide ice core chronology. Given the best  
66 quality of annual layering in WAIS Divide (as shown in figure 4) I think that the authors  
67 choose the best methodological approach to build this time scale, considering WAIS as  
68 the most reliable annually counted scale. The discussion about the uncertainty of the  
69 age scale is really well done and confirms the goodness of this first SP19 age scale  
70 both for the Holocene period (with a maximum uncertainty of about 25 years) and for  
71 older ice (maximum 124 years in the longest time window without tie points). The paper  
72 is clear and well written and I recommend its publication after considering the following  
73 minor points.

74 **Thank you.**  
75

76 Minor comments:

77 Figure 5: I would recommend to change the x-axis in kyr BP instead of using  $\times 10^4$ . In  
78 my opinion it would be much readable.

79 **We have changed the x-axis in Figure 5.**  
80

81 A list (table) of the volcanic horizons used to match WDC and SPICEcore would be  
82 valuable if inserted in the text or in supplementary material (even if archived at the  
83 NCDC or other repository).

84 **The timescale and a full list of tie points will be archived in the supplementary material and**  
85 **will be available at the National Climate Data Center ([www.ncdc.noaa.gov](http://www.ncdc.noaa.gov)) and the U.S.**  
86 **Antarctic Program Data Center (<http://www.usap-dc.org>).**  
87

88 Line 427: I would change this sentence to “Below 798 m depth (start of the  
89 Holocene): : :”

90 **Fixed.**  
91

## 92 **Review #3**

93  
94 **Thank you very much for the very useful and positive comments. We greatly**  
95 **appreciate your input. Below are our line-by-line responses to your review.**  
96

97 Review by Anders Svensson of manuscript entitled ‘The SP19 Chronology for the  
98 South Pole Ice Core – Part 1: Volcanic matching and annual-layer counting’ submitted  
99 to Climate of the Past by D. Winsky et al.

100  
101 The manuscript (MS) introduces a stratigraphic chronology SP19 of the South Pole  
102 SPICE ice core based on 1) Holocene layer counting in high-resolution discrete chemistry  
103 samples and continuous records, and 2) a transfer of the WD2014 chronology  
104 based on identification of 251 common volcanic match points distributed over the last  
105 54 ka. The layer counting is compared to a previously obtained independent layer  
106 counting from the same core based on visual stratigraphy alone. Furthermore, the  
107 authors are introducing an accumulation rate profile for the SPICE core based on a  
108 kink model. The model is compared to upstream accumulation patterns, to nitrate concentration  
109 profiles and to a d15N of N2 profile that all seem to support the obtained  
110 accumulation profile.

111  
112 Overall, the MS is well written, well referenced and the figures are clear and illustrative  
113 of the study. The MS is well structured, the language is clear and the conclusions are  
114 well argued for.

115 **Thank you.**

116  
117 I only have a few comments below for the authors to consider.  
118 The authors perform multiple careful counting of annual layers of the Holocene using  
119 chemical parameters, continuous dust and conductivity. They then compare their resulting  
120 layer counting to an independent layer counting based on visual stratigraphy  
121 alone, and find an overall good agreement between the two approaches (Figure 9).  
122 Whereas this is a good test to see how well the two independent approaches are, it  
123 would probably have resulted in a better overall time scale, if all of the available high resolution  
124 records (chemistry + visual stratigraphy) had been combined in a common  
125 dating exercise from the beginning?

126 **We agree that it would have been informative to combine the visual and chemical layer**  
127 **counting from the beginning. However, the visual layer counting was completed two years**  
128 **prior to the chemistry layer counts and had already been tied independently to WD2014**  
129 **with electrical conductivity before the chemistry data were available or before we had**  
130 **agreed on an overall dating strategy. Since the timescale was ultimately linked with**  
131 **WD2014 using sulfate and electrical conductivity, any minor changes to the timescale**  
132 **resulting from an earlier reconciliation between methods would likely have little effect and**  
133 **would be within our uncertainty estimates.**

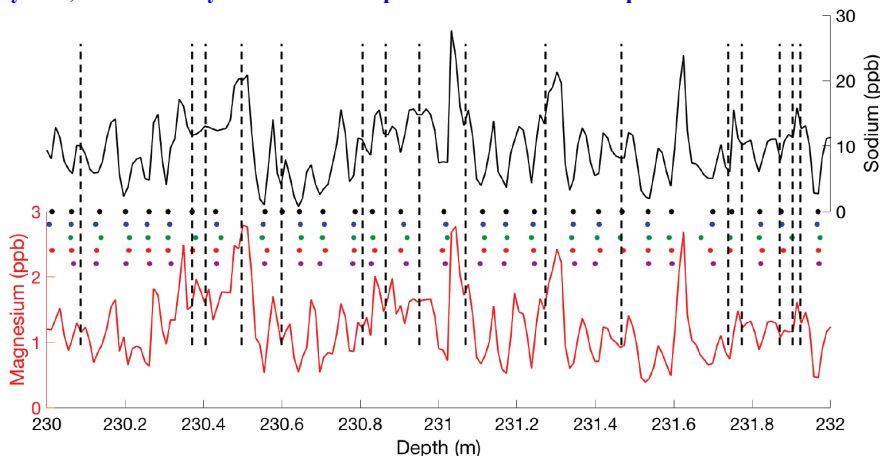
134  
135 Whereas I agree to the approach of transferring the WD2014 chronology to SPICE core  
136 rather than publishing a new independent time scale for SPICE core, it still seems like  
137 quite a large effort to do 4x independent layer counting of SPICE just to end up doing a  
138 transfer of time scale? Probably most of that time scale transfer could have been done  
139 based on a depth-depth matching alone (WDC – SPICE) similar to the approach taken  
140 in Figure 5?

141 **Yes, this was a lot of effort! We initially hoped to produce an independent timescale based**  
142 **on layer counting, but we ultimately decided to synchronize the timescale with WAIS Divide**  
143 **for the reasons described in section 3.1. However, we believe the effort was useful in**  
144 **assessing the uncertainty in the timescale.**

145  
146 There are certain depth intervals (228-275m and 626-687m), where all of the independent  
147 layer counting plus the automated Straticounter dating approach consistently

148 count significantly fewer annual layers than suggested by the transfer of the WD2014  
149 time scale. I understand that this consistent undercounting is associated with periods  
150 of exceptionally low accumulation (upstream) at SPICE. Are the authors convinced,  
151 however, that their layer counting is wrong and that there is not a problem with the  
152 WD2014 counting in one or both of those periods? In other words, can the authors  
153 account for all of the ‘missing’ layers when they go back and recount the critical sections  
154 in SPICE core? I’m not suggesting that the authors should revise the WD2014  
155 time scale, but independent checks are always useful, and considering the effort put  
156 into precise dating of SPICE, an outcome may be suggestions for future revisions of  
157 the WDC chronology?

158 **This is a good question. We were able to account for all of the ‘missing’ layers needed**  
159 **during intervals where we had initially undercounted years. During these sections, the**  
160 **annual layering was less clear and many annual layers were missed by all five interpreters.**  
161 **However, with the knowledge that there should be extra years in a given interval, it was**  
162 **never difficult to find examples of less well-expressed annual layers needed to synchronize**  
163 **the timescale. Furthermore, the missed layers often fell in intervals with smaller layer**  
164 **thickness (lower accumulation), making it difficult to resolve the annual cycle with the**  
165 **sampling frequency. The figure below shows an example of such an area near 230 m, in a**  
166 **section that was initially very undercounted. This figure is equivalent to Figure 6 in the**  
167 **manuscript with sodium and magnesium plotted against the pick positions of the 5**  
168 **interpreters. I have also added dotted lines to show where additional years were inserted**  
169 **for reconciliation. While many of the new years are poorly expressed in the chemistry or**  
170 **very thin, there is always some evidence present for each annual pick.**



171  
172

173 112,843 samples were collected and analyzed individually for this project! Did the  
174 authors consider doing fewer discrete and more continuous sample analysis? A CFA  
175 system optimized for depth/time resolution should be able to resolve the annual layering  
176 throughout the Holocene period. Of course, I’m not suggesting to do that now, but for  
177 future projects it may be an alternative?

178 **Thank you for the suggestion! It was, indeed a lot of work to process such a high volume of**  
179 **samples. Our decision to analyze discrete samples was based on previous positive**  
180 **experiences with discrete sampling, the expertise of the team and the availability of**  
181 **personnel. We believe our efforts were worthwhile due to the high quality of the resulting**

182 **data.**

183

184 A depth-difference relation figure between the two synchronized ice cores (SPICE,  
185 WDC) is very good for evaluating the synchronization and/or to identify regions where  
186 accumulation/thinning of the two records deviate. See Figure 2 of Seierstad et al.,  
187 QSR, 2014: 'Consistently dated records from the Greenland GRIP, GISP2 and NGRIP  
188 ice cores for the past 104 ka reveal regional millennial-scale d18O gradients with possible  
189 Heinrich event imprint'.

190 **Thank you for this reference. Since we have elected to tie the SP19 record exactly to the**  
191 **WD2014 record, a precisely equivalent figure would show a depth differences dominated by**  
192 **the very different accumulation rates (~7.4 cm/yr at SPICEcore and ~20 cm/yr at WAIS**  
193 **Divide) as well as very different flow patterns (SPICEcore is hundreds of kilometers from a**  
194 **divide – WAIS Divide is much closer). For instance, in WAIS Divide, 10,000 BP is located**  
195 **at 1800 meters depth – deeper than the bottom of SPICEcore. However, Fig. S1 shows some**  
196 **similar information with the age offset at a given depth between the initial, unreconciled**  
197 **layer counts with WD2014. A similar diagram to Fig. S1, or configured as done by**  
198 **Seierstad et al. 2014, in our case, would show a nearly flat line with no offset since we forced**  
199 **the timescale within +/- 1 year of each tie point.**

200

201 After having nicely synchronized the SPICE and WDC records, it would be nice to see  
202 the two climate profiles (water isotopes) in the same figure on their common time scale.  
203 If for whatever reason that is not possible, maybe the Calcium profiles of the two ice  
204 cores can be shown together? It is difficult for the reader to evaluate the quality of the  
205 volcanic matching without seeing a comparison of some parameter of the two ice core  
206 records.

207 **We have added this diagram to the supplemental material (Fig. S5) using calcium data.**

208

209 Minor comments:

210 Accumulation mistakenly used in figure 7 caption, already mentioned by Frederic.

211 **Fixed.**

212

213 In Figure 3 is shown the seasonal variability of four impurities but not including nitrate.

214 In section 4.5 and in Figure 11B the nitrate seasonality is discussed. Maybe it makes  
215 sense to include the seasonal variability of nitrate in Figure 3?

216 **We have added a 5<sup>th</sup> panel in Figure 3 to show the nitrate data.**

217

218 In Figure 7, the annual layer thickness appears to stay constant or even increase  
219 throughout the glacial part of the record. Wouldn't one normally expect a thinning  
220 of annual layering with depth?

221 **You are correct that one would expect layer thickness to decrease with depth for a constant**  
222 **accumulation rate. However, if the accumulation was higher for older ages, the extra**  
223 **thinning experienced by those will not necessarily offset the greater initial thickness. Thus,**  
224 **the layer thickness minimum near 25 ka BP could be due to accumulation rates that were**  
225 **substantially lower between 20-30 ka BP than they were beforehand. There is another**  
226 **possibility as well: the thinning function at the South Pole may be complex (i.e. not**  
227 **monotonic) due to the location hundreds of kilometers from a divide with irregular bedrock**  
228 **topography and converging/diverging flow. We have discussed Holocene accumulation**  
229 **rates here because they relate to our timescale accuracy and because they are much less**  
230 **sensitive to thinning. However, we have deliberately left a detailed interpretation of the**  
231 **layer thickness record and accumulation reconstruction for ice older than the Holocene to**  
232 **future studies (for instance Fudge et al. 2019 – CPD).**

233

233

234 The SP19 Chronology for the South Pole Ice Core - Part 1:  
235 Volcanic matching and annual-layer counting

236

237 Dominic A. Winski<sup>1,2</sup>, Tyler J. Fudge<sup>3</sup>, David G. Ferris<sup>4</sup>, Erich C. Osterberg<sup>4</sup>, John M.  
238 Fegyveresi<sup>5</sup>, Jihong Cole-Dai<sup>6</sup>, Zayta Thundercloud<sup>4</sup>, Thomas S. Cox<sup>7</sup>, Karl J. Kreutz<sup>1,2</sup>,  
239 Nikolas Ortman<sup>4</sup>, Christo Buizert<sup>8</sup>, Jenna Epifanio<sup>8</sup>, Edward J. Brook<sup>8</sup>, Ross Beaudette<sup>9</sup>,  
240 Jeff Severinghaus<sup>9</sup>, Todd Sowers<sup>10</sup>, Eric J. Steig<sup>3</sup>, Emma C. Kahle<sup>3</sup>, Tyler R. Jones<sup>11</sup>,  
241 Valerie Morris<sup>11</sup>, Murat Aydin<sup>12</sup>, Melinda R. Nicewonger<sup>12</sup>, Kimberly A. Casey<sup>13,14</sup>,  
242 Richard B. Alley<sup>10</sup>, Edwin D. Waddington<sup>3</sup>, Nels A. Iverson<sup>15</sup>, [Nelia W. Dunbar](#)<sup>15</sup>, Ryan  
243 C. Bay<sup>16</sup>, Joseph M. Souney<sup>17</sup>, [Michael Sigl](#)<sup>18</sup>, [Joseph R. McConnell](#)<sup>19</sup>

Dom Winski 8/12/19 4:12 PM  
Deleted:

244 <sup>1</sup>*School of Earth and Climate Sciences, University of Maine, Orono, Maine, USA*

245 <sup>2</sup>*Climate Change Institute, University of Maine, Orono, Maine, USA*

246 <sup>3</sup>*Department of Earth and Space Sciences, University of Washington, Seattle,  
247 Washington, USA*

248 <sup>4</sup>*Department of Earth Sciences, Dartmouth College, Hanover, New Hampshire, USA*

249 <sup>5</sup>[School of Earth and Sustainability, Northern Arizona University, Flagstaff, AZ, USA](#)

250 <sup>6</sup>*Department of Chemistry and Biochemistry, South Dakota State University, Brookings,  
251 South Dakota, USA*

252 <sup>7</sup>*Physical Science Department, Butte College, Oroville, California, USA*

253 <sup>8</sup>*College of Earth, Ocean and Atmospheric Sciences, Oregon State University, Corvallis,  
254 Oregon, USA*

255 <sup>9</sup>*Scripps Institution of Oceanography, UC San Diego, La Jolla, California, USA*

256 <sup>10</sup>*Department of Geosciences and Earth and Environmental Systems Institute,  
257 Pennsylvania State University, University Park, Pennsylvania, USA*

258 <sup>11</sup>*Institute of Arctic and Alpine Research, University of Colorado, Boulder, Colorado,  
259 USA*

260 <sup>12</sup>*Department of Earth System Science, UC Irvine, Irvine, California, USA*

261 <sup>13</sup>*Earth Sciences Division, NASA Goddard Space Flight Center, Greenbelt, MD, USA*

262 <sup>14</sup>[National Land Imaging Program, U.S. Geological Survey, Reston, VA, USA](#)

263 <sup>15</sup>*New Mexico Institute of Mining and Technology, New Mexico Bureau of Geology and  
264 Mineral Resources, Socorro, New Mexico, USA*

265 <sup>16</sup>*Physics Department, University of California, Berkeley, California, USA*

266 <sup>17</sup>*Institute for the Study of Earth, Oceans and Space, University of New Hampshire,  
267 Durham, New Hampshire, USA*

268 <sup>18</sup>[Department of Climate and Environmental Physics, University of Bern, Switzerland](#)

269 <sup>19</sup>[Division of Hydrologic Sciences, Desert Research Institute, Reno, NV, USA](#)

270

271 Correspondence to: Dominic Winski (dominic.winski@maine.edu)

272

Dom Winski 7/31/19 2:12 PM  
Deleted: U.S. Army Corps of Engineers Cold Regions Research and Engineering Laboratory, Hanover, New Hampshire

Dom Winski 7/31/19 2:10 PM  
Deleted: \*now at

## 272 Abstract

273 The South Pole Ice Core (SPICEcore) was drilled in 2014-2016 to provide a  
274 detailed multi-proxy archive of paleoclimate conditions in East Antarctica during the  
275 Holocene and late Pleistocene. Interpretation of these records requires an accurate depth-  
276 age relationship. Here, we present the SP19 timescale for the age of the ice of SPICEcore.  
277 SP19 is synchronized to the WD2014 chronology from the West Antarctic Ice Sheet  
278 Divide (WAIS Divide) ice core using stratigraphic matching of 251 volcanic events.  
279 These events indicate an age of 54,302 +/- 519 years BP (before the year 1950) at the  
280 bottom of SPICEcore. Annual layers identified in sodium and magnesium ions to 11,341  
281 BP were used to interpolate between stratigraphic volcanic tie points, yielding an  
282 annually-resolved chronology through the Holocene. Estimated timescale uncertainty  
283 during the Holocene is less than 18 years relative to WD2014, with the exception of the  
284 interval between 1800 to 3100 BP when uncertainty estimates reach +/- 25 years due to  
285 widely spaced volcanic tie points. Prior to the Holocene, uncertainties remain within 124  
286 years relative to WD2014. Results show an average Holocene accumulation rate of 7.4  
287 cm/yr (water equivalent). The time variability of accumulation rate is consistent with  
288 expectations for steady-state ice flow through the modern spatial pattern of accumulation  
289 rate. Time variations in nitrate concentration, nitrate seasonal amplitude, and  $\delta^{15}\text{N}$  of  $\text{N}_2$   
290 in turn are as expected for the accumulation-rate variations. The highly variable yet well-  
291 constrained Holocene accumulation history at the site can help improve scientific  
292 understanding of deposition-sensitive climate proxies such as  $\delta^{15}\text{N}$  of  $\text{N}_2$  and photolyzed  
293 chemical compounds.

## 294 1. Introduction

295 Polar ice core records provide rich archives of paleoclimate information that have  
296 been used to advance understanding of the climate system. One of the great strengths of  
297 ice cores is the tightly constrained dating that permits interpretation of abrupt events and  
298 comparisons of phasing among records. Therefore, a critical phase in the development of  
299 any ice core record is the rigorous establishment of a depth-age relationship.

300 Several techniques are available to assign ages to each specific depth in an ice  
301 core. These include annual layer identification of chemical (e.g. Sigl et al. 2016;  
302 Andersen et al. 2006; Winstrup et al. 2012) and physical (e.g. Hogan and Gow 1997;  
303 Alley et al. 1997) ice properties, identification of stratigraphic horizons as relative age  
304 markers (e.g. Sigl et al. 2014; Bazin et al. 2013; Veres et al. 2013) and glaciological flow  
305 modeling (e.g. Parrenin et al. 2004). To establish a depth-age relationship for the South  
306 Pole Ice Core (hereafter SPICEcore), we use a combination of 1) annual layer counting of  
307 glaciochemical tracers and 2) stratigraphic matching of volcanic horizons to the West  
308 Antarctic Ice Sheet (WAIS) Divide ice core timescale “WD2014” (Sigl et al. 2016,  
309 Buizert et al. 2015).

310 SPICEcore was drilled in 2014-2016 for the purpose of establishing proxy  
311 reconstructions of temperature, accumulation, atmospheric circulation and composition,  
312 and other earth system processes for the last 40,000 years (Casey et al. 2014). The  
313 SPICEcore record is the only ice core south of 80° S extending into the Pleistocene and is  
314 also located within one of the highest accumulation regions within interior East  
315 Antarctica (Casey et al. 2014). This provides the unique opportunity to develop the most

Dom Winski 8/13/19 10:15 AM

Deleted: 3

316 highly resolved ice core record from interior East Antarctica. The South Pole is located at  
317 | an elevation of 2835 m (Casey et al. 2014) and has a mean annual [air](#) temperature of -  
318 50°C (Lazzara et al. 2012). The high accumulation rate at South Pole (~8 cm yr<sup>-1</sup> snow  
319 water equivalent, Mosley-Thompson et al. 1999; Lilien et al. 2018) relative to most of  
320 interior East Antarctica permits glaciochemical measurements at high temporal  
321 resolution. Occasional cyclonic events, particularly during winter months, bring  
322 seasonally variable amounts of sea salt, dust and other trace chemicals to the South Pole  
323 (Ferris et al. 2011; Mosley-Thompson and Thompson 1982; Parungo et al. 1981; Hogan  
324 1997). Due to the favorable logistics and location at the geographic South Pole, the  
325 immediate area has been the site of several previous ice coring campaigns (e.g. Korotkikh  
326 et al. 2014; Budner and Cole-Dai 2003; Ferris et al. 2011; Meyerson et al. 2002; Mosley-  
327 Thompson and Thompson 1982). These ice cores contain records spanning the last two  
328 millennia, providing insight into seasonal chemistry variations and background values as  
329 well as recent snow accumulation trends.

330 In this paper, we focus on dating the ice itself; the dating of the gas record and the  
331 calculation of the gas-age/ice-age difference will be the subject of a future paper. The  
332 procedures used to generate the data necessary for ice-core dating and the dating  
333 techniques themselves are summarized in the remainder of the paper.  
334

## 335 **2. Measurements and Ice core data**

### 336 *2.1 Measurements*

337 *2.1.1 Fieldwork and Preparation* Drilling began at the South Pole in the 2014/2015  
338 austral summer season at a location 2.7 km from the Amundsen-Scott station, using the  
339 Intermediate Depth Drill designed and deployed by the U.S. Ice Drilling Program  
340 (Johnson et al. 2014). Drilling began at a depth of 5.10 m and reached a depth of 755 m  
341 in January 2015. Drilling continued during the 2015/2016 season, reaching a final depth  
342 of 1751 m. To extend the record to the surface, a 10 m core was hand-augered near the  
343 location of the main borehole. Ice core sections with a diameter of 98 mm and length of  
344 1 m were packaged and shipped to the National Science Foundation Ice Core Facility  
345 (NSF-ICF) in Denver, Colorado. Each meter-long section of core was weighed and  
346 measured to calculate density and assign core depth. The cores were cut using bandsaws  
347 into CFA (continuous flow analysis) sticks with dimensions of 24 mm x 24 mm x 1 m  
348 and packaged in clean room grade, ultra-low outgassing polyethylene layflat tubing  
349 (Texas Technologies ULO) in preparation for the melter system at Dartmouth College.  
350 An additional 13 mm x 13 mm x 1 m stick was used for water-isotope analyses at the  
351 University of Colorado (see Jones et al., 2017 for water-isotope methods).  
352

353 *2.1.2 ECM measurements* During core processing at the NSF-ICF, each core was cut and  
354 planed horizontally to produce a smooth, flat surface (Souney et al., 2014). Electrical  
355 conductivity measurements (ECM) were made with both direct current (DC) and  
356 alternating current (AC). We report only AC-ECM here, as it was the primary  
357 measurement for identifying volcanic peaks; further details are provided by Fudge et al.  
358 (2016a). Multiple tracks were made at different horizontal positions across the core  
359 (typically 3 tracks) and then averaged together. Measurements from each meter were

360 normalized by the median to preserve the volcanic signal while providing a consistent  
361 baseline conductance to account for variations in electrode contact.

362

363 2.1.3 Visual Measurements Each core was examined by JF in a dark room with  
364 illumination from below. For some cores, particularly for depths greater than ~250 m,  
365 side-directed tray lighting using a scatter-diffuser was more effective at revealing  
366 features. All noteworthy internal features, stratigraphy, physical properties and seasonal  
367 indicators were documented by hand in paper log books.

368 Previous work at the South Pole shows that coarse-grained and/or depth-hoar  
369 layers form annually in late summer, often capped by a bubble-free wind-crust or iced  
370 crust up to ~1 mm thickness (Gow, 1965). We used these coarse-grained layers as the  
371 annual “picks” (noted as late-summers). The stratigraphy in the core was generally  
372 uniform and well-preserved, with the pattern identified by Gow (1965) continuing  
373 downward. The depths of all noted features were recorded to the nearest millimeter. Full  
374 details on visual layer counting are described in Fegyveresi et al. (2019).

375

376 2.1.4. Ice Core Chemistry Analyses Ice sticks were melted and samples collected at  
377 Dartmouth College using a Continuous Flow Analysis – Discrete Sampling (CFA-DS)  
378 melt system (Osterberg et al. 2006). Stick ends were decontaminated by scraping with  
379 pre-cleaned ceramic (ZrO) knives. Cleaned sticks were then placed in pre-cleaned  
380 holders and melted on a melt head regulated by a temperature controller in a standup  
381 freezer. The melt head was made of 99.9995% pure chemical-vapor-deposited silicon  
382 carbide (CVD-SiC). CVD-SiC was chosen because of its ultra-high purity, high thermal  
383 conductivity, extreme hardness and excellent resistance to acids allowing for acid  
384 cleaning when not in use. The melt head design includes a 16x16x3 mm high tiered and  
385 rimmed inner section that was tapered with capillary slits to a center drain hole to  
386 minimize the risks of contamination from outer meltwater and wicking when melting  
387 porous firm (similar to Osterberg et al. 2006). This design provides a ≥4 mm buffer  
388 between the exterior of each ice stick and the edge of the center tiered section. Flexible  
389 plastic tines aligned on the four sides of the melt head keep the ice stick centered.

390 A peristaltic pump drew outer, contaminated meltwater away from the outer  
391 section through four waste lines. A second peristaltic pump drew clean meltwater from  
392 the center, tiered section of the melt head to a debubbler. The debubbler consisted of a  
393 short section of porous expanded PTFE tubing (Zeus Aeos 0000143895) and utilized  
394 pump pressure to force air through the tubing walls. The debubbled melt stream entered  
395 a splitter where it was separated into three fractions: one for major ion analyses, another  
396 for trace element analyses, and a third that passed through a particle counter and size  
397 analyzer (Klotz Abakus), an electrical conductivity meter (Amber Science 3084), and a  
398 flowmeter (Sensirion SLI-2000) before final collection in vials (Fig. 1). Samples were  
399 collected in cleaned vials using Gilson FC204 fraction collectors (cleaning procedures  
400 described in Osterberg et al. 2006). Samples were capped and kept frozen until  
401 additional analysis.

402 Core depths corresponding to each sample were tracked using custom software  
403 expanding on the concept of depth-point tracking developed by Breton et al. (2012).  
404 Simply, software tracks each depth point in the core as it progresses through the CFA-DS  
405 system until it reaches each collection vial. This is accomplished by using a combination

Dom Winski 8/20/19 1:37 PM

Deleted: 9

406 of melt rate, flow rates, and system line volumes. Melt rates were measured with a  
 407 weighted rotary encoder tracking displacement as the ice stick melts. Flow rates were  
 408 measured by either an electronic flow meter or by calibrating the volume per revolution  
 409 of each peristaltic pump tubing [piece](#). Fraction collector advancements were made  
 410 automatically based on melt rate, ice density (in firm), and the required sample volume  
 411 and frequency. In addition, the software collected data from the inline particle counter  
 412 and electronic conductivity meter. This system is capable of producing high-resolution,  
 413 ultra-clean samples and has been used successfully in previous studies (e.g. Osterberg et  
 414 al. 2017; Winski et al. 2017; Breton et al. 2012; Koffman et al. 2014). Samples  
 415 corresponding to the top and bottom of each stick were assigned depths equal to the top  
 416 and bottom depths measured at NSF-ICF, with intervening samples scaled linearly by the  
 417 ratio of the NSF-ICF core lengths over the lengths measured by the depth encoder. This  
 418 ensures that our data remain consistent with other SPICEcore datasets and there is no  
 419 possibility of drift due to scraping core breaks, measurement or encoder errors.

420 Discrete ion chemistry samples were collected every 1.1 cm on average for the  
 421 upper 800 m (Holocene) portion of the core and every 2.4 cm on average for older ice. In  
 422 total, 112,843 samples were collected and analyzed using a Thermo Fisher Dionex ICS-  
 423 5000 capillary ion chromatograph to determine the concentrations of the following major  
 424 ions: nitrate, sulfate, chloride, sodium, potassium, magnesium and calcium. Liquid  
 425 conductivity, particle concentration, and particle size distribution measurements were  
 426 taken continuously with an effective resolution of 3 mm.  
 427

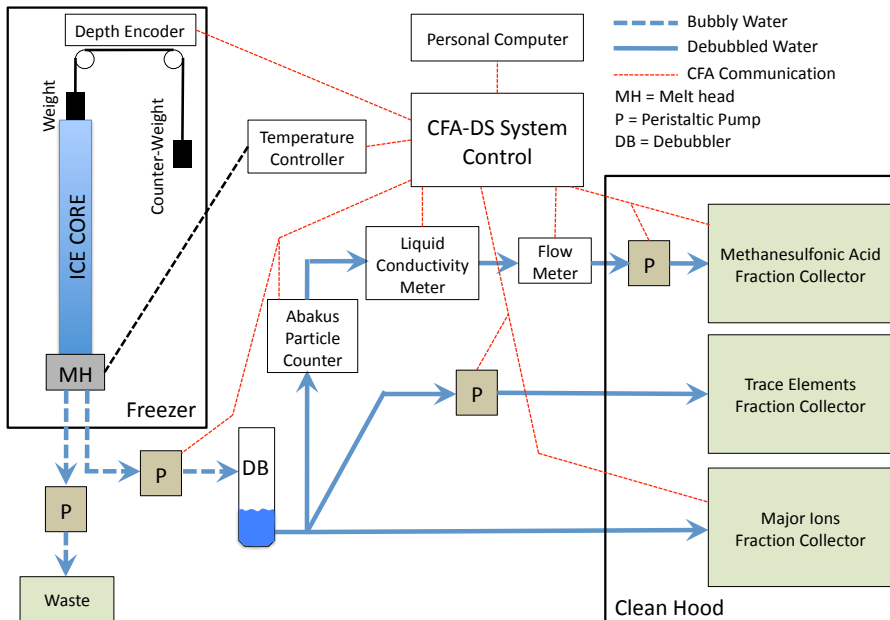


Figure 1: A schematic representation of the Dartmouth ice core melter system.

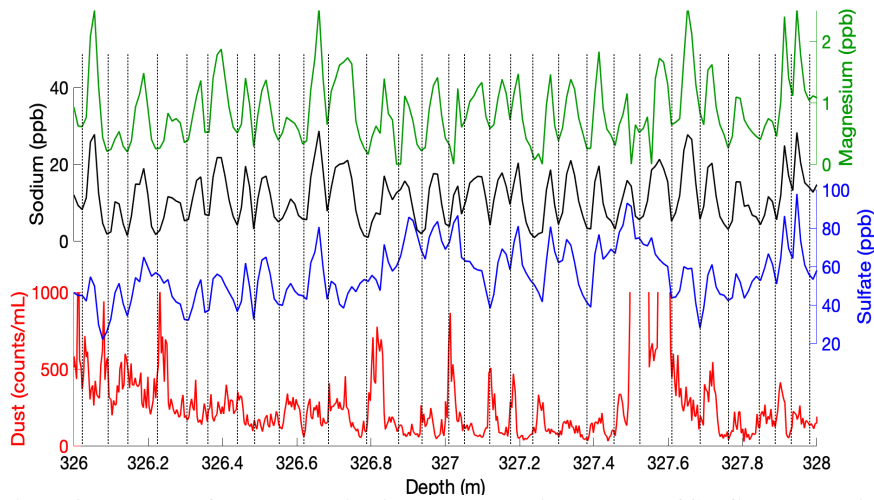
432 **2.2 Chemistry Characteristics of SPICEcore**

433

434 Previous research at the South Pole has shown that major sea salt ions ( $\text{Cl}^-$ ,  $\text{Na}^+$ ,  
435  $\text{Mg}^{2+}$ ) have winter maxima and summer minima when compared with the position of  
436 summer depth hoar layers (Cole-Dai and Mosley-Thompson 1999; Ferris et al. 2011).  
437 The same conclusion was reached through comparisons with seasonal isotopic  
438 fluctuations: sodium and magnesium peaks coincide with seasonal water-isotope minima  
439 (Legrand and Delmas 1984; Whitlow et al. 1992). These observations are consistent with  
440 sea salt aerosol measurements collected at the South Pole that demonstrate large sodium  
441 influx during winter months (Bodhaine et al. 1986; Bergin et al. 1998). The same  
442 seasonal pattern of sea salt deposition has been observed in Holocene strata of the WAIS  
443 Divide ice core (Sigl et al. 2016) and in other Antarctic ice cores (Kreutz et al. 1997;  
444 Curran et al. 1998; Wagenbach et al. 1998; Udisti et al. 2012). In the uppermost firn,  
445 seasonal chemistry is also influenced by the operation of South Pole station and its  
446 associated logistics (Casey et al. 2017).

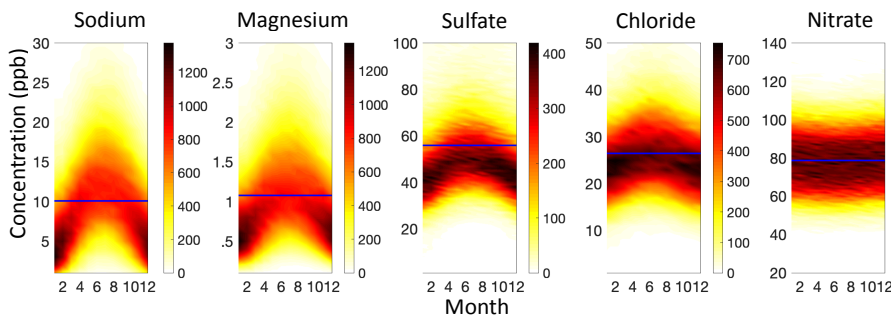
447 In SPICEcore, sampling resolution is sufficiently high to consistently detect  
448 annual cyclicality in glaciochemistry throughout the Holocene. Clear annual signals are  
449 present in several glaciochemical species to a depth of 798 m (approximately 11341 BP),  
450 with the most prominent in sodium and magnesium (Figs. 2-3), which covary ( $r = 0.95$ ;  $p$   
451  $< 0.01$ ) and have coherent annual maxima and minima. Sulfate, chloride, AC-ECM,  
452 liquid conductivity, particle count and visual stratigraphy all exhibit discernable annual  
453 cyclicality.

454 The South Pole has long been recognized as a favorable location for identifying  
455 volcanic events, reflected by previous work on South Pole paleovolcanism (Ferris et al.  
456 2011; Delmas et al. 1992; Budner and Cole-Dai 2003; Cole-Dai et al. 2009; Baroni et al.  
457 2008; Cole-Dai and Thompson 1999; Palais et al. 1990). Volcanic events in SPICEcore  
458 are evident as peaks in sulfate and ECM rising well above background values. Within the  
459 Holocene, the median annual sulfate maximum is 60 ppb. This background level  
460 increases deeper in the core to values as high as 131 ppb between 18-26 ka BP, despite  
461 the lack of annual resolution during the Pleistocene. In contrast, sulfate concentration in  
462 volcanic events regularly exceeds 200 ppb with occasional concentrations as high as 1000  
463 ppb for very large signals. For example, the pair of eruptions in 135 and 141 BP (1815  
464 and 1809 CE), attributed to Tambora and Unknown in previous Antarctic studies  
465 (Delmas et al. 1992; Cole-Dai et al. 2000; Sigl et al. 2013) have peak sulfate  
466 concentrations of 518 and 281 ppb respectively, emerging well above seasonal  
467 background values of 60 ppb.



468  
469 **Figure 2: Example of annual layering in a representative segment of SPICEcore. Depicted**  
470 **are magnesium (green) and sodium (black) concentrations showing nearly identical**  
471 **variations and clear annual cyclicality. Sulfate (blue) has consistent but less pronounced**  
472 **layering, and dust (red; 1 micron size bin) has occasionally visible annual layering. Vertical**  
473 **dashed lines show annual pick positions based on the data shown.**

474



475

476 **Figure 3: Seasonal variation in magnesium, sodium, sulfate, chloride and nitrate ion**  
477 **concentration in SPICEcore from -42 to 11341 BP (11383 total years). In each panel, the**  
478 **horizontal axis is month of the year (with 0 being Jan. 1<sup>st</sup>) from linear interpolation between**  
479 **mean sample depth and the timescale. The vertical axis is concentration (ppb). The color**  
480 **scale indicates the density of measurements within gridded month and concentration bins.**  
481 **Concentration bin widths are 1 month (without claiming 1 month precision) and 1 ppb**  
482 **except for magnesium which is 0.1 ppb. The Holocene mean concentration of each ion is**  
483 **shown as a blue bar. Strong annual cyclicality is apparent in sodium and magnesium data.**  
484 **Annual cyclicality is weaker in sulfate, chloride and nitrate data.**

485

486

487

Dom Winski 7/31/19 8:05 PM

Deleted:

Dom Winski 8/20/19 1:41 PM

Deleted: and

Dom Winski 7/31/19 7:31 PM

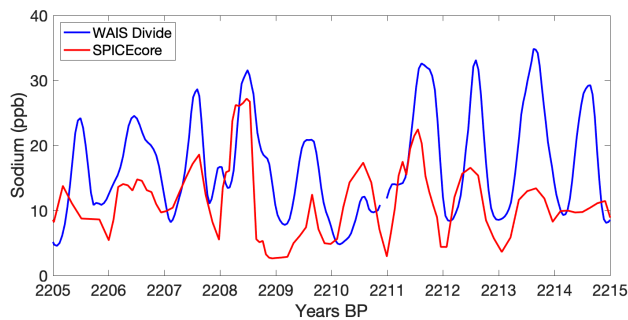
Deleted: and

488 **3. SPICEcore Dating Methods**

489 **3.1 Approach**

490 The SPICEcore timescale (SP19) was developed by combining annual layer  
491 counting with volcanic event matching between SPICEcore and the WAIS Divide  
492 chronology. We identified 251 volcanic tie points that are clearly visible in both  
493 SPICEcore and WAIS Divide (Sigl et al. 2016). These tie points link SP19 with the  
494 WAIS Divide chronology, resulting in one of the most precisely dated interior East  
495 Antarctic records. Above 798 m, ages are interpolated between volcanic tie points using  
496 layer counts. Below 798 m, ages are interpolated between tie points by finding the  
497 smoothest annual layer thickness profile (minimizing the second derivative) that satisfies  
498 at least 95% of the tie points (following Fudge et al. 2014).

499 Although it is possible to create an independent, annually layer counted  
500 SPICEcore timescale during the Holocene, we linked the entire SP19 chronology to the  
501 WAIS Divide chronology for several reasons: (1) annual layers are insufficiently thick  
502 below 798 m (approximately 11341 BP) to consistently resolve individual years,  
503 requiring synchronization to another ice core to achieve the best possible dating accuracy.  
504 Tying the entire SP19 chronology to the WAIS Divide core ensures consistent temporal  
505 relationships between these two records; (2) although annual layers are remarkably well-  
506 preserved in SPICEcore chemistry, WAIS Divide has a higher accumulation rate (Banta  
507 et al., 2008; Fudge et al., 2016b; Koutnik et al. 2016) and stronger seasonality in  
508 chemical constituents (Sigl et al. 2016), producing more robust annual layering (Figure  
509 4); (3) it is expected that some years at South Pole experience very low accumulation,  
510 resulting in a lack of an annually resolvable record during those years (Hamilton et al.  
511 2004; Van der Veen et al. 1999; Mosley-Thompson et al. 1995, 1999); (4) an attempt to  
512 independently date the Holocene annual layers created drift of several percent at  
513 stratigraphic tie points. We therefore elected to anchor the SP19 timescale to WD2014,  
514 and use the annual layer counts as a means of interpolating between WD2014 tie points  
515 during the Holocene. The SP19 timescale spans -64 BP (2014 CE) to 54,302 +/- 519 BP,  
516 with the annually-dated Holocene section of the core extending to 11341 BP (798 m  
517 depth).



518

519 | **Figure 4: Annual layering of sodium in WAIS Divide (blue; Sigl et al. 2013) and SPICEcore**  
520 **(red). Annual layers in sodium are clear in both records but are more pronounced at WAIS**  
521 **Divide for most years.**

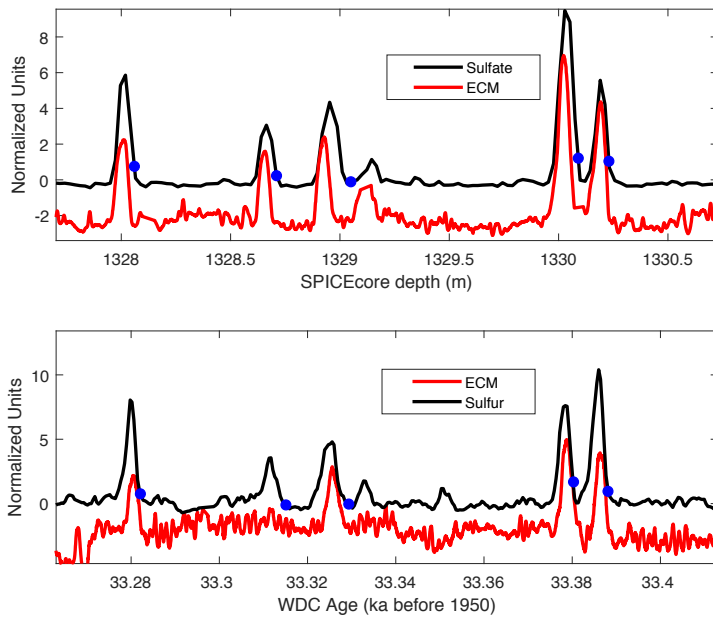
### 3.2 Procedure for identifying matching events

523 The matching of volcanic events in sulfate and ECM records is commonly used to  
524 synchronize ice core timescales (e.g. Severi et al., 2007, 2012; [Sigl et al. 2014](#); Fujita et  
525 al., 2015), including the recent extension of the annually-resolved WAIS Divide  
526 timescale to East Antarctic cores (Buizert et al., 2018). Volcanic matching is based on the  
527 depth pattern of events more than the magnitude of the events because the magnitude in  
528 individual ice cores can vary significantly across Antarctica depending on the location of  
529 the volcano and atmospheric transport to the ice core site. The volcanic matching  
530 between SPICEcore and WAIS Divide is based primarily on the sulfate record for  
531 SPICEcore and the combined sulfur and sulfate records for WAIS Divide (Buizert et al.  
532 2018). AC-ECM from SPICEcore and WAIS Divide was used as a secondary data set  
533 and to fill small data gaps in the sulfate record. An example of the four data sets is  
534 shown in Figure 5.

535 The volcanic matches were performed independently by two interpreters (TJF and DF)  
536 and then reconciled by one (TJF) with concurrence from the other (DF). The position of  
537 each match was defined as the inception of the sulfate rise in order to most consistently  
538 reflect the timing of the volcanic event itself. Of the final 251 tie points, 229 were  
539 identified in the sulfate data by both interpreters. Of the remaining matches, 14 were  
540 made by one interpreter in the sulfate data, and at least one interpreter in the ECM data.  
541 One of the other matches was made only with ECM because of a gap in the sulfate data  
542 for SPICEcore. The last 7 matches were part of sequences not initially picked by one  
543 interpreter but deemed to be sufficiently distinct from the other events in the sequence to  
544 be included.

545 We note that the purpose of the volcanic matching was to develop a robust  
546 SPICEcore timescale, not to assess volcanic forcing. Thus, there are many potential  
547 volcanic matches that were not included either because they did not have the same level  
548 of certainty as the final 251 matches, or because they were in close proximity to the final  
549 matches and thus did not provide additional timescale constraints.

550 For the pre-Holocene section of the core, ages between the volcanic matches are  
551 interpolated by finding the smoothest annual layer thickness by minimizing the second  
552 derivative (Fudge et al., 2014). The goal of finding the smoothest annual layer thickness  
553 time series is to prevent sharp changes affecting the apparent duration of climate events  
554 on either side of a volcanic match point. The method allows the ages of the volcanic  
555 matches to vary within a threshold to produce a smoother annual layer thickness  
556 interpolation. The degree of smoothness was set such that 95% of the tie points are  
557 shifted by 1-year or less, which is a reasonable uncertainty on the precision of the  
558 volcanic matches.  
559



Dom Winski 7/31/19 6:45 PM

Deleted:

560

561 **Figure 5: An example of volcanic matching between SPICEcore (top) and WAIS Divide**  
 562 **(bottom). Sulfate (black) and electrical conductivity (ECM; red) are shown for both ice**  
 563 **cores. Here, five events are shown that link specific depths in SPICEcore to known ages in**  
 564 **WAIS Divide. The position of the tie points is chosen at the beginning of the event (blue**  
 565 **circles). The y-axis values are scaled for ease of visualization and do not indicate absolute**  
 566 **measurement values.**

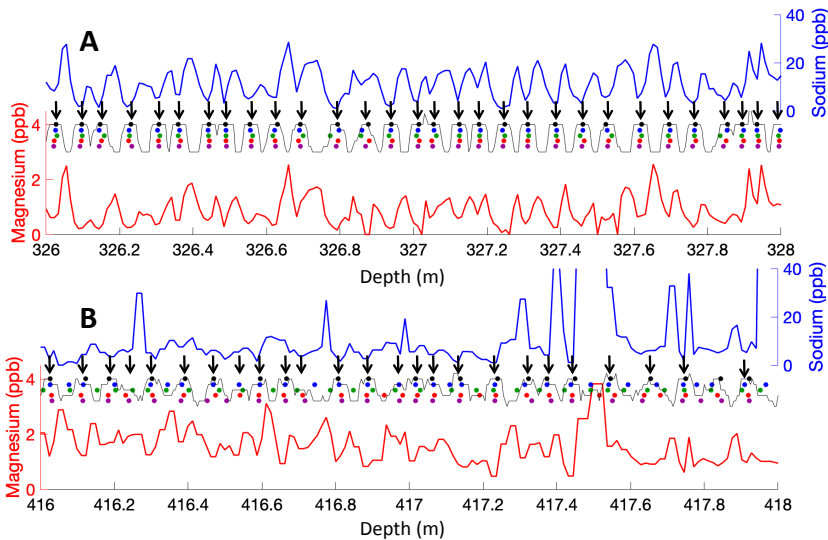
567 **3.3 Annual Layer Interpretation**

568 Annual layer counting in SPICEcore was initially done independently of the  
 569 volcanic matching with WAIS Divide. To minimize and quantify timescale uncertainty,  
 570 five interpreters performed the layer counting independently: DW, DF, TJJ, JF, and TC.  
 571 Sodium and magnesium were the primary annual indicators, but electrical conductivity,  
 572 dust concentration, sulfate, chloride and liquid conductivity were also helpful in  
 573 delineating individual years. To remain consistent, each interpreter agreed to place the  
 574 location of Jan. 1<sup>st</sup> for each year at the sodium/magnesium minimum, consistent with  
 575 previous interpretation of South Pole sea salt seasonality (e.g. Ferris et al. 2011; Bergin et  
 576 al. 1998). Two examples of annual layering including the Jan. 1<sup>st</sup> positions picked by  
 577 each interpreter are shown in Figure 6. Shown here are sections of high (A) and low (B)  
 578 agreement among the five interpreters.

579 This procedure resulted in five independent timescales to a depth of 540 m,  
 580 containing between 6529 and 6807 years. The details of reconciling the five independent  
 581 sets of layer counts are described in the Supplemental Information. Below 540 m, only  
 582 one author (DW) continued with the layer counting once the decision to use the annual  
 583 layers to interpolate between volcanic events had been made. The layer counting

584 procedure resulted in an annually resolved timescale, fully independent of any external  
585 constraints, to a depth of 798.

586 Above 798 meters, 86 volcanic tie points were identified, producing 85 intervals  
587 within which a known number of years must be present. To make the layer-counted  
588 timescale consistent with these tie points, years were added or subtracted, as necessary,  
589 within each interval such that the layer-counted timescale passed through each tie point  
590 within +/- 1 year of its age, linking SPICEcore with the WAIS divide chronology.  
591 Procedural details for adding and subtracting layers by interval are discussed in the  
592 Supplemental Information. In most intervals, few years needed to be added or subtracted,  
593 with the average change in years equal to 5.6% of the interval length (Holocene intervals  
594 ranged from 6 to 747 years). In certain sections layer counting consistently differed from  
595 the WAIS-tied timescale. The most notable example is from 228 to 275 m depth where  
596 105 years (14%) needed to be added.  
597



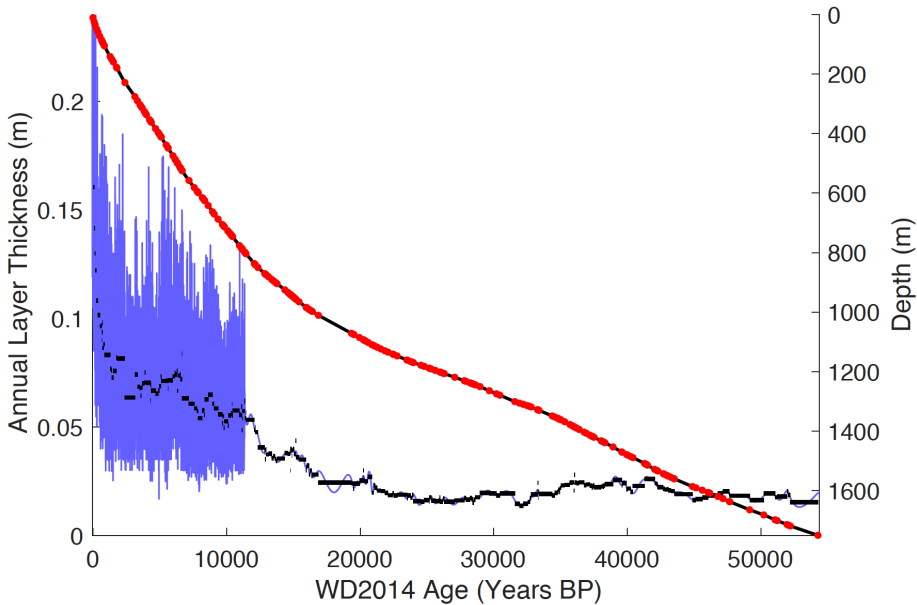
598 **Figure 6: Representative sections of annual layer pick positions compared with magnesium**  
599 **(red) and sodium (blue) concentrations. Each interpreter is represented with a different**  
600 **color circle. Certain sections have excellent agreement among interpreters making**  
601 **reconciliation trivial (A), whereas other sections have poorly defined annual signals and**  
602 **associated disagreement among interpreters (B). The black line depicts the sum of all picks**  
603 **within +/- 2 cm; black arrows depict the final positions of the reconciled Jan. 1<sup>st</sup> annual**  
604 **layer picks.**  
605  
606

## 607 4. Results and Discussion

### 608 4.1 Characteristics of the Timescale

609 The SP19 chronology extends from 2014 CE (-64 BP) at the surface to 54302 BP  
610 at 1751 m depth. The timescale and volcanic tie points are depicted in Figure 7 with  
611 volcanic tie points pinning the timescale also shown. Annual layer thicknesses near the  
612  
613

614 surface are roughly 20 cm thick (owing to the low density of firn), decreasing rapidly to  
 615 ~8 cm/yr by the firn-ice transition. The timescale is annually resolved between -64 and  
 616 11341 BP, below which resolution varies based on the distance between tie points. Using  
 617 the methods in section 3.2 (Fudge et al. 2014), we report timescale values interpolated at  
 618 10-year resolution. The longest distance between tie points is 2476 years between 16348  
 619 and 19872 BP.



620  
 621 | **Figure 7: The SP19 timescale and layer thickness. The SP19 depth-age relationship (right**  
 622 **y-axis, black line) is constrained by volcanic events (red dots) extending to 54302 BP.**  
 623 **Annual layer thicknesses (left y-axis, blue) are shown at annual resolution during the**  
 624 **Holocene and as decadal-interpolated thicknesses based on the smoothest annual layer**  
 625 **thickness method (Fudge et al. 2014) during the Pleistocene. The average annual layer**  
 626 **thickness during each volcanic interval is shown in black for comparison.**

Dom Winski 7/31/19 2:17 PM  
 Deleted: ,  
 Dom Winski 7/31/19 2:17 PM  
 Deleted: and accumulation rate

627  
 628 **4.2 Uncertainties**

629  
 630 In discussing uncertainty values for SP19, the reported values are uncertainty  
 631 *estimates* rather than rigorously quantified  $1\sigma$  or  $2\sigma$  values. There are several reasons for  
 632 this: 1) the chemicals used to count annual layers have similar cyclicity and are not  
 633 independent; 2) while each of the five interpreters counted layers independently, they  
 634 were likely employing similar strategies; 3) certain years may not be well-represented in  
 635 the data, providing insufficient information for accurate dating or quantifying  
 636 uncertainty; 4) volcanic events were identified in clusters such that each event is not  
 637 necessarily independent; 5) it is difficult to assign a numerical index of confidence to  
 638 specific volcanic tie points. Instead, we discuss timescale uncertainties as uncertainty  
 639 estimates, which are intended to approximate  $2\sigma$  uncertainties but cannot be precisely  
 640 defined as such. This approach follows that of Sigl et al. (2016).

641 We assess the SP19 timescale uncertainty with respect to the previously published  
642 WD2014 timescale (Sigl et al. 2016; Buizert et al. 2015). The absolute age uncertainty  
643 will always be equal to or greater than the uncertainty already associated with WD2014  
644 (Buizert et al. 2015; Sigl et al. 2016; Fig. 8). In addition to the uncertainty in WD2014,  
645 there is also uncertainty in our ability to interpolate between stratigraphic tie points.  
646 During the Holocene, our layer-counting of sodium and magnesium concentration  
647 improves the timescale accuracy between tie points. Interpolation uncertainty can be  
648 estimated using the drift among the five different interpreters. We calculate the number  
649 of years picked by each interpreter in running intervals of 500 years in the final WD2014  
650 synchronized timescale. Under ideal conditions, each interpreter would also pick 500  
651 years within each interval, but on average the number of years picked by interpreters  
652 differs from the final timescale by 6.7%, usually by undercounting. This is similar to the  
653 metric described in section 3.3, wherein the average change in years needed to reconcile  
654 the layer counts and volcanic tie points was 5.6% of the interval length. Here, we report  
655 the larger and more conservative value of 6.7%. If our layer counting skill drifts by +/-  
656 6.7% while unconstrained by volcanic tie points, then the interpolation uncertainties  
657 remain within +/- 18 years of WAIS Divide throughout the Holocene with the exception  
658 of a poorly-constrained interval between approximately 1800-3100 BP. The maximum  
659 uncertainty within the Holocene is +/- 25 years, occurring at roughly 2750 BP, where the  
660 nearest tie points are 373 years away at 2376 and 3123 BP. This relationship can be  
661 applied across the Holocene, with layers accumulating an uncertainty value equal to 6.7%  
662 of the distance to the nearest tie point (Fig. 8; blue).

663 | Below 798 m depth ([start of the Holocene](#)), there were no annual layers to aid in  
664 our interpolation of the timescale, leading to larger uncertainties. Our assumption of the  
665 smoothest annual layer thickness (Fudge et al. 2014) satisfying tie points is the most  
666 accurate interpolation method in the absence of additional information, at least in  
667 Antarctic ice (Fudge et al. 2014). Using the WAIS Divide ice core as a test case, Fudge  
668 et al. (2014) estimated that the interpolation method accumulates uncertainties at a rate of  
669 10% of the distance to the nearest tie-point, roughly 50% faster than the uncertainty of  
670 periods with identifiable annual layers. The longest interval with no volcanic constraints  
671 is between 16348 and 19872 BP. At 18110 BP, the center of the interval, the  
672 interpolation uncertainty reaches a maximum of 124 years, although uncertainties are  
673 | proportionally lower in other intervals with closer volcanic tie points.

674 Figure 8 shows the total uncertainty estimates associated with the SP19  
675 chronology, with interpolation uncertainties added to the published WAIS Divide  
676 uncertainties. The WD2014 and interpolation uncertainties are added in quadrature since  
677 the two sources of uncertainty are independent. The maximum estimated uncertainty in  
678 SP19 is 533 years at 34050 BP, the majority of which is attributed to uncertainties in  
679 WD2014. While it is not possible to rigorously quantify uncertainties throughout SP19,  
680 we believe these estimates provide reasonable and conservative values suitable for most  
681 paleoclimate applications. We acknowledge there is additional uncertainty related to the  
682 accuracy of our assigned stratigraphic tie points. Because of the conservative procedures  
683 discussed in section 3.1 wherein only unambiguous matches were used in linking the  
684 WAIS Divide and SPICEcore timescales, it is unlikely that any of these matches are in  
685 error. In previous work (Ruth et al. 2007), potential errors associated with tie points have  
686 been estimated by removing each tie point one at a time, and interpolating between the

Dom Winski 7/31/19 6:47 PM

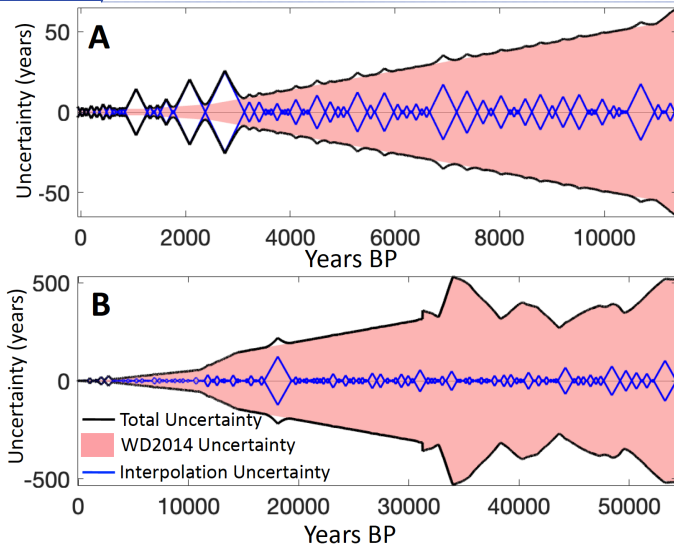
Deleted: the Holocene (

Dom Winski 7/31/19 6:47 PM

Deleted: )

687 new series of tie points (with one point missing). If this procedure is repeated for each  
 688 point and for each depth, the maximum error in age resulting from the erroneous  
 689 inclusion of a tie point is approximately 83 years. However, because clusters of volcanic  
 690 events were used to match the WAIS Divide and SPICEcore records, each tie point is not  
 691 necessarily independent. Therefore, this method is more useful at sections of widely  
 692 spaced tie points with greater potential uncertainties, but underestimates the uncertainties  
 693 surrounding closely spaced events in SPICEcore and WAIS Divide. [Examining calcium](#)  
 694 [records from WAIS Divide \(Markle et al. 2018\) and SPICEcore shows concurrent timing](#)  
 695 [in calcium variations between the two cores \(Fig. S5\), further supporting the choices of](#)  
 696 [tie points.](#)

Dom Winski 8/13/19 10:05 AM  
 Deleted:



697 **Figure 8: Uncertainty estimates in the SP19 timescale. The pink shading indicates the**  
 698 **published uncertainty associated with the WAIS Divide timescale (Buizert et al., 2015; Sigl**  
 699 **et al., 2016). The blue lines indicate the estimated uncertainty due to interpolation by layer**  
 700 **counting (Holocene) and by finding the smoothest annual layer thickness history (Fudge et**  
 701 **al. 2014; Pleistocene). Total uncertainty (black) is defined here as the root sum of the**  
 702 **squares of the interpolation and WD2014 uncertainties. Total uncertainty estimates remain**  
 703 **within +/- 50 years for most of the Holocene (A), but are as high as 533 years in the**  
 704 **Pleistocene (B).**

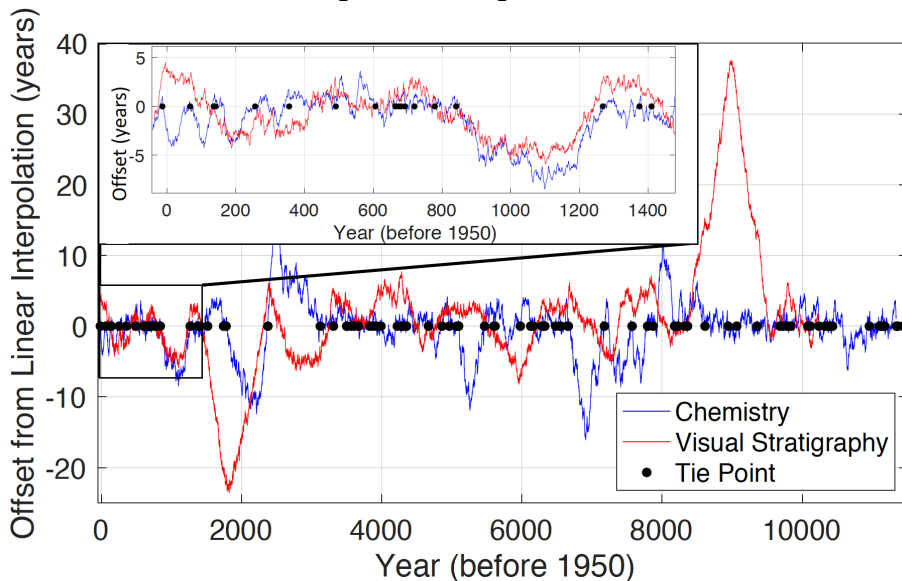
### 706 4.3 Comparison with Visual Stratigraphy

707 Visual stratigraphy in SPICEcore provides an independent check on the  
 708 glaciochemical layer counting we used to interpolate the Holocene depth-age scale  
 709 between tie points. Visual layer counting was conducted to a depth of 735 m (~10,250  
 710 years BP; Fegyveresi et al. 2017). We calculate the offset between the visual stratigraphic  
 711 timescale and a linear interpolation between tie points and do the same for the chemistry  
 712 layer counts (Fig. 9). If both the chemical and visual layer counting methods are  
 713 capturing the true variability in layer thickness within intervals, then both would show the  
 714 same structure within each interval.  
 715  
 716

717 There is broad correspondence between visual and chemical stratigraphy at all  
 718 depths, which, with their almost completely independent origin and measurements  
 719 techniques, is highly reassuring. In detail, though, there is little high-frequency  
 720 correspondence between visible and chemical layer counts below 1400 BP (150 m depth),  
 721 although a direct comparison is not possible since visible layer counts were not linked to  
 722 stratigraphic tie points between 1400-2400 BP and 8400-9500 BP. Furthermore, visible  
 723 layer counts were matched to the tie points within error of the WAIS Divide timescale,  
 724 whereas the chemistry layer counts were forced to match within +/- 1 year of each tie  
 725 point. In counting visible layers, occasional under- and overcounting of depth hoar layers  
 726 within annual strata is likely, especially in deeper ice where thinning will make adjacent  
 727 layers appear even closer. There were some intervals (e.g. 2000 – 2500 BP) in the core  
 728 that appeared more homogeneous during viewing, and therefore annual layer choices  
 729 have a higher level of uncertainty. Because of the differences between methodologies in  
 730 matching to tie points and because of the uncertainties in visual counting below 2000 BP  
 731 (200 m), we did not attempt to reconcile the visible and chemical layer counts, but  
 732 instead rely only on the annual layers in the chemistry data.

Dom Winski 7/31/19 6:27 PM  
 Deleted:

733 Between 100 and 1400 BP, both visible and glaciochemical timescales remain  
 734 remarkably coherent and do not indicate drift of more than +/- 2 years. Over this interval,  
 735 the correlation between the visible and chemical layer offsets from constant annual layer  
 736 thickness (red and blue curves in Figure 9) is 0.74. The correlation between the two layer  
 737 counting methods is as high as  $r = 0.85$  between the tie points at 841 and 1268 BP. The  
 738 discrepancy within the top 100 years is due to the tie point at 10.58 m, which was not  
 739 included at the time of visible layer counting, as well as low layer chemical counting  
 740 confidence within the firn column. There is no obvious relation between the  
 741 accumulation rate and statistical agreement among methods.



742  
 743 **Figure 9: Comparison between visible layer (red) and chemistry-based (blue) Holocene**  
 744 **annual timescales. Both curves are shown as residual values with respect to a linear**

745 interpolation between tie points (black circles). When the shape of the red and blue curves  
746 is similar between tie points, we infer relatively high accuracy in both methods. The region  
747 showing the closest agreement between methods is shown in the inset with both curves  
748 remaining within 2 years of each other despite a long section with no tie points (841 to 1286  
749 BP).

#### 750 4.4 Accumulation Rate History

751 The SP19 timescale allows us to produce annually-resolved estimates of past  
752 snow accumulation to 11341 BP (Fig. 10). We apply a Dansgaard-Johnsen model  
753 (Dansgaard et al. 1969) to estimate the amount of thinning undergone by each layer of  
754 ice. Since the entirety of the Holocene in SPICEcore is located within the top third of the  
755 core (over 1900 m above the bed), the challenges associated with reconstructing surface  
756 accumulation are smaller than at sites with records closer to the bed (e.g. Kaspari et al.  
757 2008, Thompson et al. 1998, Winski et al. 2017). Radar measurements indicate a bed  
758 depth at the South Pole of 2812 m, giving an ice-equivalent thickness of 2774 m, using  
759 the South Pole density function developed by Kuivinen et al. (1982). We used a kink  
760 height of 20% of the ice thickness and an input surface accumulation rate of 8 cm/yr  
761 (water equivalent), consistent with the parameters used by Lilien et al. (2018). The  
762 average Holocene accumulation rate is 7.4 cm/yr (water equivalent), in excellent  
763 agreement with results of previous studies (Hogan and Gow 1997; 7.5 cm/yr to 2000 BP;  
764 Mosley-Thompson et al. 1999 – 6.5-8.5 cm/yr for late 20<sup>th</sup> century). The upstream flow  
765 dynamics are too complicated for a static 1-D model to accurately determine the thinning  
766 function before the Holocene.  
767

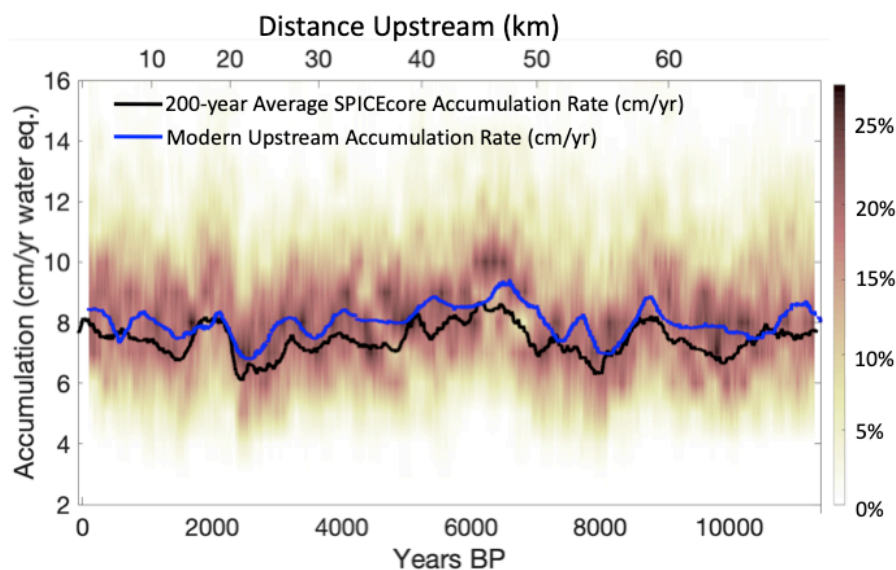
768 As discussed in Lilien et al. (2018), Koutnik et al. (2016), and Waddington et al.  
769 (2007), South Pole layer thicknesses are affected by 1) spatial variability in surface  
770 accumulation being advected to South Pole; 2) past climate-related changes in snow  
771 accumulation; and 3) post-depositional thinning due to ice flow. Thinning models can  
772 account for only the third factor. Understanding of Holocene climate history as recorded  
773 at other sites and in other indicators in SPICEcore, combined with knowledge of the  
774 modern upglacier variation in accumulation (Lilien et al., 2018), make it clear that the  
775 Holocene SPICEcore time-variations in accumulation are primarily from advection of  
776 spatial variations. Figure 10 shows Holocene accumulation rate in SPICEcore (black)  
777 compared with geophysically derived accumulation estimates over space using ice-  
778 penetrating radar (blue, details in Lilien et al. 2018). Using the present-day surface  
779 velocity field and the inferred 15% increase in flow rate, present day upstream surface  
780 accumulation rates were matched with corresponding ages at the SPICEcore borehole  
781 (Lilien et al. 2018). The close match between present-day near-surface accumulation  
782 rates upstream and the annual accumulation rate in SPICEcore shows that the millennial-  
783 scale signal of accumulation rate in SPICEcore is related to spatial patterns of snow  
784 accumulation upstream of South Pole.

Dom Winski 7/31/19 6:28 PM

Deleted:

Dom Winski 7/31/19 6:28 PM

Deleted:



785  
 786 **Figure 10: The Holocene accumulation rate history in SPICEcore. Shading indicates a**  
 787 **running histogram of accumulation rate with darker colors indicative of more years at a**  
 788 **given accumulation rate. The color axis (left) indicates percentage of years with a given**  
 789 **accumulation rate within 1 cm accumulation bins across 200-year sliding intervals. The**  
 790 **solid black line is the 200-year running mean of accumulation rate. These data are**  
 791 **compared with modern spatial accumulation rates upstream of SPICEcore (blue; upper x-**  
 792 **axis; Lilien et al. 2018).**

793 A striking feature in the Holocene accumulation record in SPICEcore is the sharp  
 794 dip centered on 2400 BP. Annual layers were notably less clear in that portion of  
 795 SPICEcore because low accumulation rates led to low sampling resolution (5-6  
 796 samples/year). For instance, in the interval between 228-275 m, the interpreters picked  
 797 between 511 and 670 years, when 747 years are present based on the volcanic tie points.  
 798 [Because the undercounting of layers in the development of SP19 is coincident with low](#)  
 799 [accumulation rates, we are confident that this undercounting is due to poorly resolved](#)  
 800 [layers in SPICEcore rather than to erroneous tie points or errors in the WD2014](#)  
 801 [chronology.](#)

802 The cause of the sharp drop in accumulation is not clear. Modern accumulation  
 803 rates upstream of SPICEcore were measured using a 20 m-deep isochron imaged with ice  
 804 penetrating radar (Lilien et al. 2018). These results show lower accumulation in the  
 805 location where the 2400 BP ice originated (Fig. 10). However, the modern upstream  
 806 spatial pattern of accumulation shows a decline that is both more gradual and less than  
 807 half the magnitude of the 2400 BP change in SPICEcore. It is possible that this represents  
 808 a climatic signal, but we note sharp accumulation variations at this time that are not  
 809 observed in the WAIS Divide core (Fudge et al. 2016b; Koutnik et al. 2016). Instead, we  
 810 hypothesize that this event was most likely a transient local accumulation anomaly.  
 811 Farther upstream at ~75km from South Pole, there is an accumulation low where the rate  
 812 of change is approximately 3 cm/yr in 2 km. With the current South Pole ice flow

813 velocity of 10 m/yr, this could explain a 3 cm/yr decrease in 200 years, similar to what is  
814 observed at 2400 BP. If a climate-driven accumulation anomaly did contribute to this  
815 sharp change, these anomalies do not appear to be common, as we see no other large and  
816 sustained change in the annual timescale.

817 On sub-centennial timescales, the effects of upstream advection of spatial  
818 accumulation patterns are likely smaller, such that annual-to-decadal patterns in snow  
819 accumulation in SPICEcore may be indicative of climate conditions. Previous studies  
820 have used a snow stake field 400 m to the east (upwind) of South Pole station to assess  
821 recent trends in accumulation rate with differing results. Mosley-Thompson et al. (1995,  
822 1999) found a trend of increasing snow accumulation during the late 20<sup>th</sup> century, while  
823 Monaghan et al. (2006) and Lazzara et al. (2012) found decreasing snow accumulation  
824 trends between 1985-2005 and 1983-2010, respectively. No significant trends exist in the  
825 SPICEcore accumulation record within the last 50 years, although there is a significant ( $p$   
826 = 0.046) increasing trend in snow accumulation in SPICEcore since 1900. Note that  
827 errors in measured firn density would influence this accumulation trend.

828

#### 829 **4.5 Nitrate Variability, $\delta^{15}N$ of $N_2$ , and Accumulation**

830

831 SPICEcore nitrate concentrations provide independent support for the Holocene  
832 accumulation rate history implied by the SP19 timescale. Previous studies have  
833 recognized an association between accumulation rate and nitrate concentration among ice  
834 core sites (Rothlisberger et al. 2002). Nitrate in surface snow, exposed to sunlight, results  
835 in photolytic reactions that volatilize nitrate and release it to the atmosphere (Erland et  
836 al. 2013, Grannas et al. 2007; Rothlisberger et al. 2000). Evaporation of  $HNO_3$  may also  
837 significantly contribute to nitrate loss in the surface snow (Munger et al. 1999; Grannas et  
838 al. 2007). Under low-accumulation conditions such as in East Antarctica, the amount of  
839 time snow is exposed at the surface is the dominant control on nitrate concentration, such  
840 that with more accumulation, snow is more rapidly buried and retains higher nitrate  
841 concentrations (Rothlisberger et al. 2000).

842 There is close correspondence between accumulation rate and nitrate  
843 concentration in SPICEcore (Fig. 11A). This association is strongest on multidecadal to  
844 multicentennial timescales with correlation coefficients between accumulation rate and  
845 nitrate reaching peak values after 512-year smoothing ( $r = 0.60$ ; Fig. 11 inset). Although  
846 the smoothing makes standard metrics of statistical significance inapplicable, the  
847 similarity between time series is expected given the previous work described above.  
848 Among sites, an inverse relationship exists between seasonal amplitude of nitrate  
849 concentration and accumulation rate. High-accumulation sites such as Summit,  
850 Greenland exhibit strong annual nitrate layering, whereas low-accumulation sites such as  
851 Vostok (~2 cm w.e./yr; Ekaykin et al. 2004) and Dome C (~3.6 cm w.e./yr; Petit et al.  
852 1982) do not show annual nitrate layers at all (Rothlisberger et al. 2000). SPICEcore has  
853 much higher accumulation rates than Vostok or Dome C, and retains weak intra-annual  
854 variability in nitrate. While minor compared with multi-annual and longer variability,  
855 nitrate seasonal cyclicality, wherein nitrate often peaks in the summer months, (described in  
856 Grannas et al. 2007; Davis et al. 2004) is discernable in the SPICEcore nitrate record. As  
857 expected, the seasonal amplitude of nitrate over the Holocene closely follows nitrate  
858 concentration and accumulation rate (Figure 11B) and is even more highly correlated

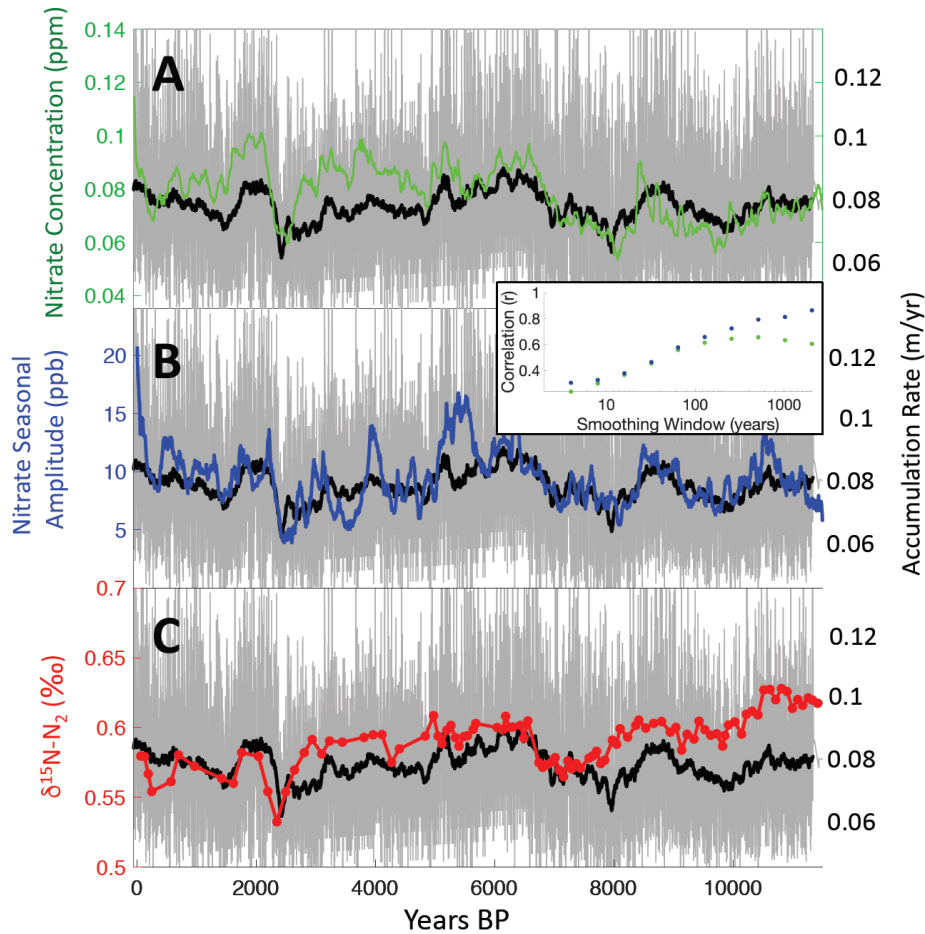
Dom Winski 7/31/19 7:25 PM

**Deleted:** seasonality

Dom Winski 7/31/19 7:26 PM

**Deleted:** , the mechanisms for which are complex

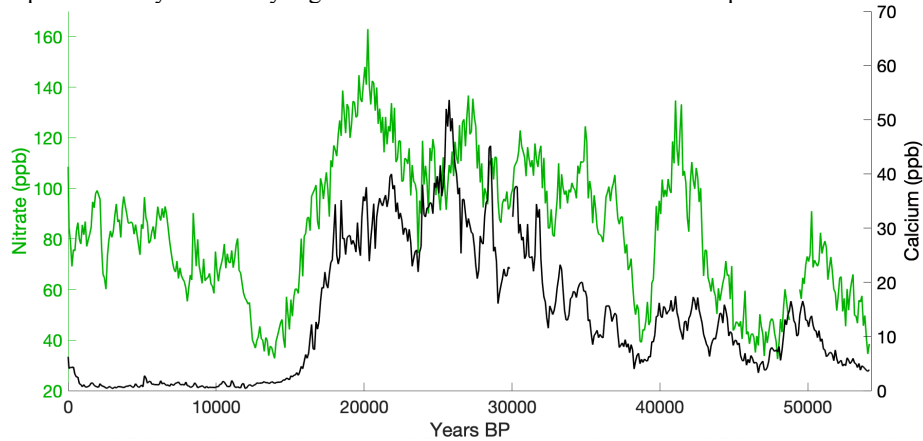
859 with accumulation than nitrate concentration itself, especially on multicentennial to  
 860 millennial timescales ( $r = 0.80$  at 512-year smoothing). Nitrate and accumulation rate are  
 861 entirely independent variables in terms of their measurement, adding confidence to the  
 862 annual layer counting and tie points underlying the SP19 chronology.



863  
 864 **Figure 11: The Holocene accumulation rate at the South Pole compared with nitrate and**  
 865  **$\delta^{15}\text{N}-\text{N}_2$ .** In each panel, annual accumulation rates are depicted in gray, with the running  
 866 **100-year mean shown in black.** These results are compared with 100-year median annual  
 867 **values of nitrate concentration (A) and seasonal amplitude in nitrate concentration (B) as**  
 868 **well as  $\delta^{15}\text{N}-\text{N}_2$  values (C).** All three metrics exhibit shared variability on multicentennial to  
 869 **millennial timescales.** The inset shows the correlation between accumulation rate and  
 870 **nitrate concentration (green) from panel A, and between accumulation rate and nitrate**  
 871 **seasonal amplitude (blue) from panel B, against length of the smoothing window, with both**  
 872 **exhibiting high correlations, especially at lower frequencies.**

873  
 874 The relationship between inferred variations in accumulation rate and nitrate

875 concentration breaks down prior to the Holocene, but a relationship between nitrate and  
 876 calcium concentrations emerges. During the Pleistocene, the correlation between  
 877 centennial median of calcium and nitrate is  $r = 0.80$  ( $p < 0.01$ ; Figure 12), compared with  
 878  $r = 0.26$  ( $p < 0.01$ ) during the Holocene. Rothlisberger et al. (2000, 2002) observed the  
 879 same pattern at Dome C, and attributed it to the stabilization of nitrate through interaction  
 880 with calcium and dust. They proposed that  $\text{CaCO}_3$  and  $\text{HNO}_3$  react to form  $\text{Ca}(\text{NO}_3)_2$ ,  
 881 which is more resistant to photolysis and consequently leads to higher concentrations of  
 882 nitrate in the glacial age snowpack despite lower accumulation rates. The stabilization  
 883 effect of calcium apparently overtakes photolysis and evaporation of nitrate in terms of  
 884 importance only at the very high calcium concentrations as seen in the pre-Holocene ice.

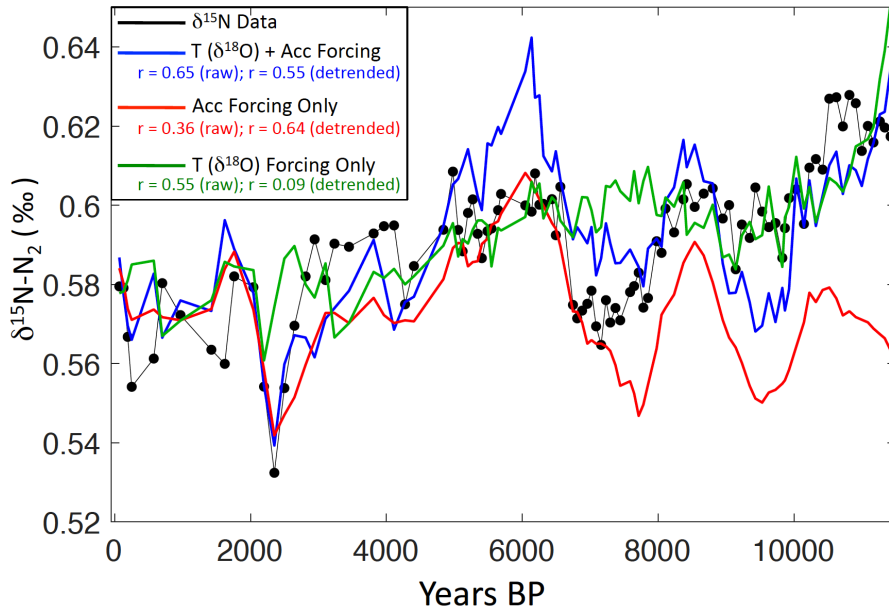


885  
 886 **Figure 12: Nitrate and calcium concentrations in SPICEcore. There is low centennial-scale**  
 887 **correlation ( $r = 0.26$ ;  $p < 0.01$ ) between calcium and nitrate ions during the Holocene, when**  
 888 **accumulation is the dominant control on nitrate concentration (Fig. 11). During the**  
 889 **Pleistocene, centennial median nitrate and calcium are positively correlated ( $r = 0.80$ ;  $p <$**   
 890  **$0.01$ ).**

891  
 892 Stable isotope ratios of atmospheric diatomic nitrogen ( $\delta^{15}\text{N-N}_2$ ) in trapped air in  
 893 SPICEcore show a pattern similar to accumulation rate within the Holocene (Fig. 11C).  
 894  $\delta^{15}\text{N-N}_2$  values were measured using the procedures described by Petrenko et al. (2006).  
 895 The  $\delta^{15}\text{N-N}_2$  in ice cores is driven by gravitational enrichment and is a proxy for past  
 896 thickness of the firn column (Sowers et al 1992). Firn densification rates depend  
 897 primarily on temperature and overburden pressure, with the second parameter closely  
 898 linked to the accumulation rate at the site. Low temperatures and high accumulation rates  
 899 both act to thicken the firn, thereby increasing  $\delta^{15}\text{N-N}_2$  (Herron and Langway 1980,  
 900 Goujon 2003).

901 We perform a simple attribution study to see whether  $\delta^{15}\text{N-N}_2$  variations can be  
 902 explained by reconstructed accumulation history or variable temperature. We compare  
 903 three climatic scenarios in a dynamical version of the Herron-Langway densification  
 904 model (Buizert et al. 2014). The first uses variable temperature (from  $\delta^{18}\text{O}$  using a  
 905 scaling ratio of  $0.8\text{‰}/^\circ\text{C}$ ) and variable accumulation (from annual layer thickness)  
 906 forcing; a second uses constant temperature ( $-51.5^\circ\text{C}$ ) and the variable accumulation  
 907 forcing; a third uses variable temperature and constant accumulation ( $7.8\text{ cm/yr}$ ) forcing.

908 The correlations between the  $\delta^{15}\text{N-N}_2$  data and each model run are displayed in Fig. 13  
 909 for both raw and detrended time series. The model scenario forced by both temperature  
 910 and accumulation has the best correspondence with the  $\delta^{15}\text{N-N}_2$  data ( $r = 0.65$ ;  $p < 0.01$ ).  
 911 While secular changes in temperature appear to be driving the decreasing trend in  $\delta^{15}\text{N-N}_2$ -  
 912  $\text{N}_2$ , millennial-scale fluctuations in  $\delta^{15}\text{N-N}_2$  appear to be driven by accumulation,  
 913 supported by the high correlation ( $r = 0.64$ ;  $p < 0.01$ ) with the accumulation-only model  
 914 run using detrended time series. In particular, a sharp drop in  $\delta^{15}\text{N-N}_2$  is present at  
 915 approximately 2400 BP, coincident with (and driven by) the local minimum in  
 916 accumulation. These experiments provide additional confidence in the reconstructed  
 917 accumulation history. To our knowledge, these data represent the best observation of  
 918 accumulation-driven  $\delta^{15}\text{N-N}_2$  variation, making it a valuable target for benchmarking firm  
 919 densification model performance (Lundin et al. 2017).



920  
 921 | **Figure 13: Results from three firm models compared with  $\delta^{15}\text{N-N}_2$  variations in SPICEcore**  
 922 | **(black). The model run incorporating only  $\delta^{18}\text{O}$ -based temperature (green) does not**  
 923 | **capture the millennial-scale variations in  $\delta^{15}\text{N-N}_2$ , whereas the models using only**  
 924 | **accumulation (red) and both accumulation and  $\delta^{18}\text{O}$ -based temperature (blue) are able to**  
 925 | **reproduce the observed millennial-scale  $\delta^{15}\text{N-N}_2$  changes. Correlations between the  $\delta^{15}\text{N-N}_2$**   
 926 | **data and the three model runs are reported in the legend with correlation coefficients**  
 927 | **calculated for both raw and linearly detrended time series.**  
 928

Dom Winski 8/20/19 1:48 PM  
 Deleted:

929 **5. Summary**

930 The SP19 includes the last 54,366 (-64 to 54,302 BP) years, and is the oldest and  
 931 most well-constrained ice core timescale from the South Pole. SP19 was developed using

932 251 volcanic events that link the SPICEcore timescale with the WAIS Divide chronology  
933 WD2014 (Sigl et al. 2016; Buizert et al. 2015). High-resolution chemical records in  
934 SPICEcore during the Holocene provide the only annually resolved full-Holocene  
935 paleoclimate record in interior East Antarctica. Within the Holocene, SP19 uncertainties  
936 are in the range of +/- 18 years with respect to WAIS Divide, with the exception of the  
937 interval between 1800-3100 BP when low accumulation and sparse volcanic controls lead  
938 to uncertainties as high as +/- 25 years. During the Pleistocene, SP19 uncertainties are  
939 inversely related to the density of tie points, with maximum uncertainties reaching +/-  
940 124 years relative to WD2014. Results show an average Holocene accumulation rate of  
941 7.4 cm/yr with millennial-scale variations that are closely linked with advection of spatial  
942 surface-accumulation patterns upstream of the drill site. Nitrate concentrations, nitrate  
943 seasonal amplitude, and  $\delta^{15}\text{N-N}_2$  variability are positively correlated with accumulation  
944 rate during the Holocene, providing independent confirmation of the SP19 chronology.

## 945 **Competing Interests**

946 The authors declare that they have no conflict of interest.

## 947 **Data Availability**

948 The SP19 chronology, associated tie points, uncertainty estimates and supporting data  
949 sets will be archived at the National Climate Data Center ([www.ncdc.noaa.gov](http://www.ncdc.noaa.gov)) and the  
950 U.S. Antarctic Program Data Center (<http://www.usap-dc.org>) with the publication of this  
951 paper.

## 952 **Author Roles**

953 All authors contributed data to this study. DW, DF, EO, JCD, ZT, KK, and NO  
954 measured the ice core chemistry. TJF and EDW collected the ECM data. JF and RA  
955 performed the visual analysis. CB, JE, EB, RB, JS, JF and TS made the gas  
956 measurements. ES, EK, TJ, and VM made the isotope measurements. DW, TJF, DF, JF  
957 and TC performed the annual layer counting. TJF and DF performed the volcanic  
958 matching. DW, TJF, DF, EO, JF and CB wrote the paper with contributions from all  
959 authors.

## 960 **Acknowledgements**

961 This work was funded through U.S. National Science Foundation grants 1443105,  
962 1141839 (Steig), 1443336 (Osterberg), 1443397 (Kreutz), 1443663 (Cole-Dai), 1443232  
963 (Waddington, Fudge), 1142517, 1443470 (Aydin), 1443464 (Sowers), 1443710  
964 (Severinghaus), 1542778 (Alley, Fegyveresi), 1443472, 1643722 (Brook), [1543454](#)  
965 ([Dunbar](#)). We thank Mark Twickler and the SPICEcore Science Coordination Office for  
966 administering the project; the U.S. Ice Drill Program Office for recovering the ice core;  
967 the 109th New York Air National Guard for airlift in Antarctica; the field team who  
968 helped collect the core; the members of South Pole station who facilitated the field  
969 operations; National Science Foundation Ice Core Facility for ice core processing; and  
970 the many student researchers who produced the data underlying the SP19 timescale.  
971

Dom Winski 8/12/19 4:13 PM

Formatted: Font:Times New Roman

Dom Winski 8/20/19 1:50 PM

Deleted:

972 **References**

- 973 Alley, R. B., Shuman, C. A., Meese, D. A., Gow, A. J., Taylor, K. C., Cuffey, K. M., Fitzpatrick,  
974 J. J., Grootes, P. M., Zielinski, G. A., and Ram, M.: Visual-stratigraphic dating of the GISP2 ice  
975 core: Basis, reproducibility, and application, *Journal of Geophysical Research: Oceans*, 102,  
976 26367-26381, 1997.
- 977 Andersen, K. K., Svensson, A., Johnsen, S. J., Rasmussen, S. O., Bigler, M., Röthlisberger, R.,  
978 Ruth, U., Siggaard-Andersen, M.-L., Steffensen, J. P., and Dahl-Jensen, D.: The Greenland ice  
979 core chronology 2005, 15–42 ka. Part 1: constructing the time scale, *Quat. Sci. Rev.*, 25, 3246-  
980 3257, 2006.
- 981 Banta, J. R., McConnell, J. R., Frey, M. M., Bales, R. C., and Taylor, K.: Spatial and temporal  
982 variability in snow accumulation at the West Antarctic Ice Sheet Divide over recent centuries,  
983 *Journal of Geophysical Research: Atmospheres*, 113, 2008.
- 984 Baroni, M., Savarino, J., Cole-Dai, J., Rai, V. K., and Thiemens, M. H.: Anomalous sulfur  
985 isotope compositions of volcanic sulfate over the last millennium in Antarctic ice cores, *Journal*  
986 *of Geophysical Research: Atmospheres*, 113, 2008.
- 987 Bazin, L., Landais, A., Lemieux-Dudon, B., Kele, H. T. M., Veres, D., Parrenin, F., Martinerie,  
988 P., Ritz, C., Capron, E., and Lipenkov, V.: An optimized multi-proxy, multi-site Antarctic ice and  
989 gas orbital chronology (AICC2012): 120-800 ka, *Clim. Past.*, 9, 1715-1731, 2013.
- 990 Bergin, M. H., Meyerson, E. A., Dibb, J. E., and Mayewski, P. A.: Relationship between  
991 continuous aerosol measurements and firn core chemistry over a 10-year period at the South Pole,  
992 *Geophys. Res. Lett.*, 25, 1189-1192, 1998.
- 993 Bodhaine, B. A., Deluisi, J. J., Harris, J. M., Houmere, P., and Bauman, S.: Aerosol  
994 measurements at the South Pole, *Tellus B: Chemical and Physical Meteorology*, 38, 223-235,  
995 1986.
- 996 Breton, D. J., Koffman, B. G., Kurbatov, A. V., Kreutz, K. J., and Hamilton, G. S.: Quantifying  
997 signal dispersion in a hybrid ice core melting system, *Environ. Sci. Technol.*, 46, 11922-11928,  
998 2012.
- 999 Budner, D., and Cole-Dai, J.: The number and magnitude of large explosive volcanic eruptions  
1000 between 904 and 1865 AD: Quantitative evidence from a new South Pole ice core, *Volcanism*  
1001 *and the Earth's Atmosphere*, 165-176, 2003.
- 1002 Buizert, C., Cuffey, K. M., Severinghaus, J. P., Baggenstos, D., Fudge, T. J., Steig, E. J., Markle,  
1003 B. R., Winstrup, M., Rhodes, R. H., and Brook, E. J.: The WAIS Divide deep ice core WD2014  
1004 chronology—Part 1: Methane synchronization (68–31 ka BP) and the gas age–ice age difference,  
1005 *Clim. Past.*, 11, 153-173, 2015.
- 1006 Buizert, C., Gkinis, V., Severinghaus, J. P., He, F., Lecavalier, B. S., Kindler, P., Leuenberger,  
1007 M., Carlson, A. E., Vinther, B., and Masson-Delmotte, V.: Greenland temperature response to  
1008 climate forcing during the last deglaciation, *Science*, 345, 1177-1180, 2014.

1009 Buizert, C., Sigl, M., Severi, M., Markle, B. R., Wettstein, J. J., McConnell, J. R., Pedro, J. B.,  
1010 Sodemann, H., Goto-Azuma, K., and Kawamura, K.: Abrupt ice-age shifts in southern westerly  
1011 winds and Antarctic climate forced from the north, *Nature*, 563, 681, 2018.

1012 Casey, K. A., Fudge, T. J., Neumann, T. A., Steig, E. J., Cavitte, M. G. P., and Blankenship, D.  
1013 D.: The 1500 m South Pole ice core: recovering a 40 ka environmental record, *Ann. Glaciol.*, 55,  
1014 137-146, 2014.

1015 Casey, K. A., Kaspari, S. D., Skiles, S. M., Kreutz, K., and Handley, M. J.: The spectral and  
1016 chemical measurement of pollutants on snow near South Pole, Antarctica, *Journal of Geophysical  
1017 Research: Atmospheres*, 122, 6592-6610, 2017.

1018 Cole-Dai, J., and Mosley-Thompson, E.: The Pinatubo eruption in South Pole snow and its  
1019 potential value to ice-core paleovolcanic records, *Ann. Glaciol.*, 29, 99-105, 1999.

1020 Cole-Dai, J., Ferris, D., Lanciki, A., Savarino, J., Baroni, M., and Thiemens, M. H.: Cold decade  
1021 (AD 1810–1819) caused by Tambora (1815) and another (1809) stratospheric volcanic eruption,  
1022 *Geophys. Res. Lett.*, 36, 2009.

1023 Cole-Dai, J., Mosley-Thompson, E., Wight, S. P., and Thompson, L. G.: A 4100-year record of  
1024 explosive volcanism from an East Antarctica ice core, *Journal of Geophysical Research:  
1025 Atmospheres*, 105, 24431-24441, 2000.

1026 Curran, M. A. J., Van Ommen, T. D., and Morgan, V.: Seasonal characteristics of the major ions  
1027 in the high-accumulation Dome Summit South ice core, Law Dome, Antarctica, *Ann. Glaciol.*,  
1028 27, 385-390, 1998.

1029 Dansgaard, W., and Johnsen, S. J.: A flow model and a time scale for the ice core from Camp  
1030 Century, Greenland, *J. Glaciol.*, 8, 215-223, 1969.

1031 Davis, D., Chen, G., Buhr, M., Crawford, J., Lenschow, D., Lefler, B., Shetter, R., Eisele, F.,  
1032 Mauldin, L., and Hogan, A.: South Pole NO<sub>x</sub> chemistry: an assessment of factors controlling  
1033 variability and absolute levels, *Atmos. Environ.*, 38, 5375-5388, 2004.

1034 Delmas, R. J., Kirchner, S., Palais, J. M., and Petit, J. R.: 1000 years of explosive volcanism  
1035 recorded at the South Pole, *Tellus B*, 44, 335-350, 1992.

1036 Ekaykin, A. A., Lipenkov, V. Y., Kuzmina, I. N., Petit, J. R., Masson-Delmotte, V., and Johnsen,  
1037 S. J.: The changes in isotope composition and accumulation of snow at Vostok station, East  
1038 Antarctica, over the past 200 years, *Ann. Glaciol.*, 39, 569-575, 2004.

1039 Erbland, J., Vicars, W. C., Savarino, J., Morin, S., Frey, M. M., Frosini, D., Vince, E., and  
1040 Martins, J. M. F.: Air–snow transfer of nitrate on the East Antarctic Plateau—Part 1: Isotopic  
1041 evidence for a photolytically driven dynamic equilibrium in summer, *Atmos. Chem. Phys.*, 13,  
1042 6403-6419, 2013.

1043 Fegyveresi, J. M., Fudge, T. J., Winski, D. A., Ferris, D. G., Alley R. B.: Visual Observations and  
1044 Stratigraphy of the South Pole Ice Core (SPICEcore): A Chronology, ERDC/CRREL Report No.  
1045 TR-19-10. ERDC-CRREL Hanover, NH, United States, 10.21079/11681/33378, 2019.

1046

Dom Winski 7/31/19 2:08 PM  
**Formatted:** Font:Not Bold, Font color: Auto

Dom Winski 7/31/19 2:07 PM  
**Deleted:** 7

Dom Winski 7/31/19 2:08 PM  
**Formatted:** Font:Times New Roman, 11 pt, Not Bold, Font color: Auto

Dom Winski 7/31/19 2:08 PM  
**Formatted:** Font:Not Bold, Font color: Auto

Dom Winski 7/31/19 2:08 PM  
**Formatted:** Font color: Auto

- 1047 Ferris, D. G., Cole-Dai, J., Reyes, A. R., and Budner, D. M.: South Pole ice core record of  
 1048 explosive volcanic eruptions in the first and second millennia AD and evidence of a large  
 1049 eruption in the tropics around 535 AD, *J. Geophys. Res.-Atmos.*, 116, 10.1029/2011jd015916,  
 1050 2011.
- 1051 Fudge, T. J., Taylor, K. C., Waddington, E. D., Fitzpatrick, J. J., and Conway, H.: Electrical  
 1052 stratigraphy of the WAIS Divide ice core: Identification of centimeter-scale irregular layering,  
 1053 *Journal of Geophysical Research: Earth Surface*, 121, 1218-1229, 2016a.
- 1054 Fudge, T. J., Markle, B. R., Cuffey, K. M., Buizert, C., Taylor, K. C., Steig, E. J., Waddington, E.  
 1055 D., Conway, H., and Koutnik, M.: Variable relationship between accumulation and temperature  
 1056 in West Antarctica for the past 31,000 years, *Geophys. Res. Lett.*, 43, 3795-3803, 2016b.
- 1057 Fudge, T. J., Waddington, E. D., Conway, H., Lundin, J. M. D., and Taylor, K.: Interpolation  
 1058 methods for Antarctic ice-core timescales: application to Byrd, Siple Dome and Law Dome ice  
 1059 cores, *Clim. Past.*, 10, 1195-1209, 2014.
- 1060 Fujita, S., Parrenin, F., Severi, M., Motoyama, H., and Wolff, E. W.: Volcanic synchronization of  
 1061 Dome Fuji and Dome C Antarctic deep ice cores over the past 216 kyr, *Clim. Past.*, 11, 1395-  
 1062 1416, 2015.
- 1063 Goujon, C., Barnola, J. M., and Ritz, C.: Modeling the densification of polar firn including heat  
 1064 diffusion: Application to close-off characteristics and gas isotopic fractionation for Antarctica and  
 1065 Greenland sites, *Journal of Geophysical Research: Atmospheres*, 108, 2003.
- 1066 Gow, A. J.: On the accumulation and seasonal stratification of snow at the South Pole, *J. Glaciol.*,  
 1067 5, 467-477, 1965.
- 1068 Grannas, A. M., Jones, A. E., Dibb, J., Ammann, M., Anastasio, C., Beine, H. J., Bergin, M.,  
 1069 Bottenheim, J., Boxe, C. S., and Carver, G.: An overview of snow photochemistry: evidence,  
 1070 mechanisms and impacts, *Atmos. Chem. Phys.*, 7, 4329-4373, 2007.
- 1071 Hamilton, G. S.: Topographic control of regional accumulation rate variability at South Pole and  
 1072 implications for ice-core interpretation, *Ann. Glaciol.*, 39, 214-218, 2004.
- 1073 Herron, M. M., and Langway, C. C.: Firn densification: an empirical model, *J. Glaciol.*, 25, 373-  
 1074 385, 1980.
- 1075 Hogan, A.: A synthesis of warm air advection to the South Polar Plateau, *Journal of Geophysical  
 1076 Research: Atmospheres*, 102, 14009-14020, 1997.
- 1077 Hogan, A. W., and Gow, A. J.: Occurrence frequency of thickness of annual snow accumulation  
 1078 layers at South Pole, *Journal of Geophysical Research: Atmospheres*, 102, 14021-14027, 1997.
- 1079 Johnson, J. A., Shturmakov, A. J., Kuhl, T. W., Mortensen, N. B., and Gibson, C. J.: Next  
 1080 generation of an intermediate depth drill, *Ann. Glaciol.*, 55, 27-33, 2014.
- 1081 Jones, T. R., White, J. W. C., Steig, E. J., Vaughn, B. H., Morris, V., Gkinis, V., Markle, B. R.,  
 1082 and Schoenemann, S. W.: Improved methodologies for continuous-flow analysis of stable water  
 1083 isotopes in ice cores, *Atmospheric Measurement Techniques*, 10, 2017.

- 1084 Kaspari, S., Hooke, R. L., Mayewski, P. A., Kang, S., Hou, S., and Qin, D.: Snow accumulation  
 1085 rate on Qomolangma (Mount Everest), Himalaya: synchronicity with sites across the Tibetan  
 1086 Plateau on 50–100 year timescales, *J. Glaciol.*, 54, 343-352, 2008.
- 1087 Koffman, B. G., Kreutz, K. J., Breton, D. J., Kane, E. J., Winski, D. A., Birkel, S. D., Kurbatov,  
 1088 A. V., and Handley, M. J.: Centennial-scale variability of the Southern Hemisphere westerly wind  
 1089 belt in the eastern Pacific over the past two millennia, *Clim. Past.*, 10, 1125-1144, 2014.
- 1090 Korotkikh, E. V., Mayewski, P. A., Dixon, D., Kurbatov, A. V., and Handley, M. J.: Recent  
 1091 increase in Ba concentrations as recorded in a South Pole ice core, *Atmos. Environ.*, 89, 683-687,  
 1092 2014.
- 1093 Koutnik, M. R., Fudge, T. J., Conway, H., Waddington, E. D., Neumann, T. A., Cuffey, K. M.,  
 1094 Buizert, C., and Taylor, K. C.: Holocene accumulation and ice flow near the West Antarctic Ice  
 1095 Sheet Divide ice core site, *Journal of Geophysical Research: Earth Surface*, 121, 907-924, 2016.
- 1096 Kreutz, K. J., Mayewski, P. A., Meeker, L. D., Twickler, M. S., Whitlow, S. I., and Pittalwala, II:  
 1097 Bipolar changes in atmospheric circulation during the Little Ice Age, *Science*, 277, 1294-1296,  
 1098 10.1126/science.277.5330.1294, 1997.
- 1099 Kuivinen, K. C., Koci, B. R., Holdsworth, G. W., and Gow, A. J.: South Pole ice core drilling,  
 1100 1981–1982, *Antarct. JUS*, 17, 89-91, 1982.
- 1101 Lazzara, M. A., Keller, L. M., Markle, T., and Gallagher, J.: Fifty-year Amundsen–Scott South  
 1102 Pole station surface climatology, *Atmos. Res.*, 118, 240-259, 2012.
- 1103 Legrand, M. R., and Delmas, R. J.: The ionic balance of Antarctic snow: a 10-year detailed  
 1104 record, *Atmospheric Environment (1967)*, 18, 1867-1874, 1984.
- 1105 Lilien, D., Fudge, T. J., Koutnik, M., Conway, H., Osterberg, E., Ferris, D., Waddington, E.,  
 1106 Stevens, C. M., and Welten, K. C.: Holocene ice-flow speedup in the vicinity of South Pole,  
 1107 [Journal of Geophysical Research](#), 2018.
- 1108 Lundin, J. M. D., Stevens, C. M., Arthern, R., Buizert, C., Orsi, A., Ligtenberg, S. R. M.,  
 1109 Simonsen, S. B., Cummings, E., Essery, R., and Leahy, W.: Firm Model Intercomparison  
 1110 Experiment (FirmMICE), *J. Glaciol.*, 63, 401-422, 2017.
- 1111 [Markle, B. R., Steig, E. J., Roe, G. H., Winckler, G., McConnell, J. R., Concomitant variability in](#)  
 1112 [high-latitude aerosols, isotopes, and the hydrologic cycle, Nature Geoscience, 2018.](#)
- 1113 Meyerson, E. A., Mayewski, P. A., Kreutz, K. J., Meeker, L. D., Whitlow, S. I., and Twickler, M.  
 1114 S.: The polar expression of ENSO and sea-ice variability as recorded in a South Pole ice core, in:  
 1115 *Annals of Glaciology*, Vol 35, edited by: Wolff, E. W., *Annals of Glaciology*, 430-436, 2002.
- 1116 Monaghan, A. J., Bromwich, D. H., Fogt, R. L., Wang, S.-H., Mayewski, P. A., Dixon, D. A.,  
 1117 Ekaykin, A., Frezzotti, M., Goodwin, I., and Isaksson, E.: Insignificant change in Antarctic  
 1118 snowfall since the International Geophysical Year, *Science*, 313, 827-831, 2006.
- 1119 Mosley-Thompson, E., Kruss, P. D., Thompson, L. G., Pourchet, M., and Grootes, P.: Snow  
 1120 stratigraphic record at South Pole: potential for paleoclimatic reconstruction, *Ann. Glaciol.*, 7, 26-  
 1121 33, 1985.

Dom Winski 8/3/19 6:42 PM  
 Deleted: submitted

- 1122 Mosley-Thompson, E., Paskievitch, J. F., Gow, A. J., and Thompson, L. G.: Late 20th Century  
1123 increase in South Pole snow accumulation, *J. Geophys. Res.-Atmos.*, 104, 3877-3886,  
1124 10.1029/1998jd200092, 1999.
- 1125 Mosley-Thompson, E., and Thompson, L. G.: Nine Centuries of Microparticle Deposition at the  
1126 South Pole 1, *Quat. Res.*, 17, 1-13, 1982.
- 1127 Mosley-Thompson, E., Thompson, L. G., Paskievitch, J. F., Pourchet, M., Gow, A. J., Davis, M.  
1128 E., and Kleinman, J.: Recent increase in South Pole snow accumulation, *Ann. Glaciol.*, 21, 131-  
1129 138, 1995.
- 1130 Munger, J. W., Jacob, D. J., Fan, S. M., Colman, A. S., and Dibb, J. E.: Concentrations and  
1131 snow-atmosphere fluxes of reactive nitrogen at Summit, Greenland, *Journal of Geophysical*  
1132 *Research: Atmospheres*, 104, 13721-13734, 1999.
- 1133 Osterberg, E. C., Handley, M. J., Sneed, S. B., Mayewski, P. A., and Kreutz, K. J.: Continuous  
1134 ice core melter system with discrete sampling for major ion, trace element, and stable isotope  
1135 analyses, *Environ. Sci. Technol.*, 40, 3355-3361, 10.1021/es052536w, 2006.
- 1136 Osterberg, E. C., Winski, D. A., Kreutz, K. J., Wake, C. P., Ferris, D. G., Campbell, S., Introne,  
1137 D., Handley, M., and Birkel, S.: 1200-Year Composite Ice Core Record of Aleutian Low  
1138 Intensification, *Geophys. Res. Lett.*, 2017.
- 1139 Palais, J. M., Kirchner, S., and Delmas, R. J.: Identification of some global volcanic horizons by  
1140 major element analysis of fine ash in Antarctic ice, *Ann. Glaciol.*, 14, 216-220, 1990.
- 1141 Parrenin, F., Remy, F., Ritz, C., Siegert, M. J., and Jouzel, J.: New modeling of the Vostok ice  
1142 flow line and implication for the glaciological chronology of the Vostok ice core, *Journal of*  
1143 *Geophysical Research: Atmospheres*, 109, 2004.
- 1144 Parungo, F., Bodhaine, B., and Bortniak, J.: Seasonal variation in Antarctic aerosol, *Journal of*  
1145 *aerosol science*, 12, 491-504, 1981.
- 1146 Petit, J. R., Jouzel, J., Pourchet, M., and Merlivat, L.: A detailed study of snow accumulation and  
1147 stable isotope content in Dome C (Antarctica), *Journal of Geophysical Research: Oceans*, 87,  
1148 4301-4308, 1982.
- 1149 Petrenko, V. V., Severinghaus, J. P., Brook, E. J., Reeh, N., and Schaefer, H.: Gas records from  
1150 the West Greenland ice margin covering the Last Glacial Termination: a horizontal ice core,  
1151 *Quat. Sci. Rev.*, 25, 865-875, 2006.
- 1152 Röthlisberger, R., Hutterli, M. A., Sommer, S., Wolff, E. W., and Mulvaney, R.: Factors  
1153 controlling nitrate in ice cores: Evidence from the Dome C deep ice core, *Journal of Geophysical*  
1154 *Research: Atmospheres*, 105, 20565-20572, 2000.
- 1155 Röthlisberger, R., Hutterli, M. A., Wolff, E. W., Mulvaney, R., Fischer, H., Bigler, M., Goto-  
1156 Azuma, K., Hansson, M. E., Ruth, U., and Siggaard-Andersen, M.-L.: Nitrate in Greenland and  
1157 Antarctic ice cores: a detailed description of post-depositional processes, *Ann. Glaciol.*, 35, 209-  
1158 216, 2002.
- 1159 Ruth, U., Barnola, J. M., Beer, J., Bigler, M., Blunier, T., Castellano, E., Fischer, H., Fundel, F.,  
1160 Huybrechts, P., and Kaufmann, P.: "EDML1": a chronology for the EPICA deep ice core from

- 1161 Dronning Maud Land, Antarctica, over the last 150 000 years, *Climate of the Past Discussions*, 3,  
1162 549-574, 2007.
- 1163 Severi, M., Becagli, S., Castellano, E., Morganti, A., Traversi, R., Udisti, R., Ruth, U., Fischer,  
1164 H., Huybrechts, P., and Wolff, E.: Synchronisation of the EDML and EDC ice cores for the last  
1165 52 kyr by volcanic signature matching, *Climate of the Past Discussions*, 3, 409-433, 2007.
- 1166 Severi, M., Udisti, R., Becagli, S., Stenni, B., and Traversi, R.: Volcanic synchronisation of the  
1167 EPICA-DC and TALDICE ice cores for the last 42 kyr BP, *Clim. Past.*, 8, 509-517, 2012.
- 1168 Severinghaus, J. P., Sowers, T., Brook, E. J., Alley, R. B., and Bender, M. L.: Timing of abrupt  
1169 climate change at the end of the Younger Dryas interval from thermally fractionated gases in  
1170 polar ice, *Nature*, 391, 141, 1998.
- 1171 Sigl, M., Fudge, T. J., Winstrup, M., Cole-Dai, J., Ferris, D., McConnell, J. R., Taylor, K. C.,  
1172 Welten, K. C., Woodruff, T. E., and Adolphi, F.: The WAIS Divide deep ice core WD2014  
1173 chronology—Part 2: Annual-layer counting (0–31 ka BP), *Clim. Past.*, 12, 769-786, 2016.
- 1174 [Sigl, M., McConnell, J.R., Toohey, M., Curran, M., Das, S.B., Edwards, R., Isaksson, E.,  
1175 Kawamura, K., Kipfstuhl, S., Krüger, K., Layman, L., Maselli, O.J., Motizuki, Y., Motoyama, H.,  
1176 Pasteris, D.R. and Severi, M., 2014. Insights from Antarctica on volcanic forcing during the  
1177 Common Era. \*Nature Climate Change\*, 4\(8\): 693-697.](#)
- 1178 Sigl, M., McConnell, J. R., Layman, L., Maselli, O., McGwire, K., Pasteris, D., Dahl-Jensen, D.,  
1179 Steffensen, J. P., Vinther, B., Edwards, R., Mulvaney, R., and Kipfstuhl, S.: A new bipolar ice  
1180 core record of volcanism from WAIS Divide and NEEM and implications for climate forcing of  
1181 the last 2000 years, *J. Geophys. Res.-Atmos.*, 118, 1151-1169, 10.1029/2012jd018603, 2013.
- 1182 Souney, J. M., Twickler, M. S., Hargreaves, G. M., Bencivengo, B. M., Kippenhan, M. J.,  
1183 Johnson, J. A., Cravens, E. D., Neff, P. D., Nunn, R. M., and Orsi, A. J.: Core handling and  
1184 processing for the WAIS Divide ice-core project, *Ann. Glaciol.*, 55, 15-26, 2014.
- 1185 Sowers, T., Bender, M., Raynaud, D., and Korotkevich, Y. S.:  $\delta^{15}\text{N}$  of  $\text{N}_2$  in air trapped in polar  
1186 ice: A tracer of gas transport in the firn and a possible constraint on ice age-gas age differences,  
1187 *Journal of Geophysical Research: Atmospheres*, 97, 15683-15697, 1992.
- 1188 Thompson, L. G., Davis, M. E., Mosley-Thompson, E., Sowers, T. A., Henderson, K. A.,  
1189 Zagorodnov, V. S., Lin, P. N., Mikhalenko, V. N., Campen, R. K., and Bolzan, J. F.: A 25,000-  
1190 year tropical climate history from Bolivian ice cores, *Science*, 282, 1858-1864, 1998.
- 1191 Torrence, C., and Compo, G. P.: A practical guide to wavelet analysis, *Bull. Amer. Meteorol.*  
1192 *Soc.*, 79, 61-78, 1998.
- 1193 Udisti, R., Dayan, U., Becagli, S., Busetto, M., Frosini, D., Legrand, M., Lucarelli, F., Preunkert,  
1194 S., Severi, M., and Traversi, R.: Sea spray aerosol in central Antarctica. Present atmospheric  
1195 behaviour and implications for paleoclimatic reconstructions, *Atmos. Environ.*, 52, 109-120,  
1196 2012.
- 1197 van der Veen, C. J., Mosley-Thompson, E., Gow, A. J., and Mark, B. G.: Accumulation At South  
1198 Pole: Comparison of two 900-year records, *J. Geophys. Res.-Atmos.*, 104, 31067-31076,  
1199 10.1029/1999jd900501, 1999.

- 1200 Veres, D., Bazin, L., Landais, A., Toyé Mahamadou Kele, H., Lemieux-Dudon, B., Parrenin, F.,  
1201 Martinerie, P., Blayo, E., Blunier, T., and Capron, E.: The Antarctic ice core chronology  
1202 (AICC2012): an optimized multi-parameter and multi-site dating approach for the last 120  
1203 thousand years, *Clim. Past.*, 9, 1733-1748, 2013.
- 1204 Waddington, E. D., Neumann, T. A., Koutnik, M. R., Marshall, H.-P., and Morse, D. L.:  
1205 Inference of accumulation-rate patterns from deep layers in glaciers and ice sheets, *J. Glaciol.*, 53,  
1206 694-712, 2007.
- 1207 Wagenbach, D., Ducroz, F., Mulvaney, R., Keck, L., Minikin, A., Legrand, M., Hall, J. S., and  
1208 Wolff, E. W.: Sea-salt aerosol in coastal Antarctic regions, *Journal of Geophysical Research:*  
1209 *Atmospheres*, 103, 10961-10974, 1998.
- 1210 Whitlow, S., Mayewski, P. A., and Dibb, J. E.: A comparison of major chemical species seasonal  
1211 concentration and accumulation at the South Pole and Summit, Greenland, *Atmospheric*  
1212 *Environment. Part A. General Topics*, 26, 2045-2054, 1992.
- 1213 Winski, D., Osterberg, E. F., D. Kreutz, K., Wake, C. C., S. Hawley, R., Roy, S., and Birkel, S. I.,  
1214 D. Handley, M.: Industrial-age doubling of snow accumulation in the Alaska Range linked to  
1215 tropical ocean warming, *Nature Scientific Reports*, 2017.
- 1216 Winstrup, M., Svensson, A. M., Rasmussen, S. O., Winther, O., Steig, E. J., and Axelrod, A. E.:  
1217 An automated approach for annual layer counting in ice cores, *Clim. Past*, 8, 1881-1895,  
1218 10.5194/cp-8-1881-2012, 2012.
- 1219

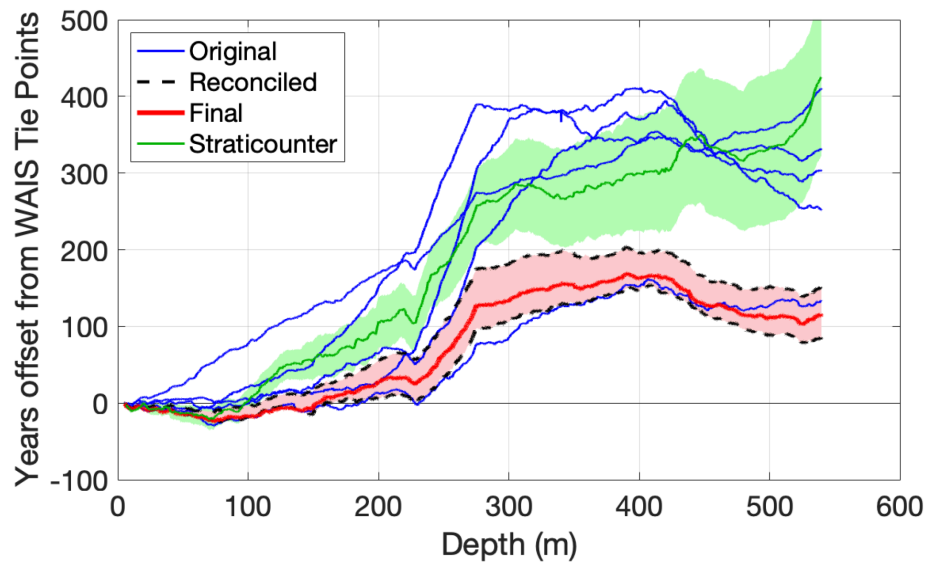
## 1219 Supplemental Information

### 1220 S1. Annual Layer Counting Methods

1221 Layer counting was done in two phases. The first phase spans 5 to 540 m depth  
1222 and the second phase includes 540 to 798 m depth. The specific annual-layer counting  
1223 procedure is described for each phase.

#### 1224 *S1.1 Layer Counting from 5-540 meters*

1225 Above 540 m, all five interpreters independently picked annual layers using the  
1226 glaciochemical time series described above. These efforts resulted in five separate  
1227 timescales. Over the top 540 m of SPICEcore, the different interpreters identified  
1228 between 6529 and 6807 years, with sometimes inconsistent offsets between the  
1229 interpreters. These five timescales are plotted in Figure S1 with respect to a timescale  
1230 passing through each of the tie points developed in section 3.2, with positive values  
1231 indicating that layer counts are missing in order to synchronize ages with WAIS Divide  
1232 (blue lines). To combine the 5 sets of timescales into a single unified timescale, we first  
1233 identified clusters of individual layer picks. For depths above 540 m, we calculated the  
1234 sum of the number of individual layer picks within a moving window +/- 2 cm wide at  
1235 0.5 cm increments. In an ideal scenario, with all 5 researchers picking a layer in the same  
1236 position, reconciliation among the sets of picks is simple (Fig. 6A). However, in some  
1237 areas choosing between the 5 sets of picks is non-trivial (Fig. 6B). DW and DF  
1238 individually and independently reviewed the five sets of picks using independently  
1239 established criteria to decide whether each cluster of picks represented a year for  
1240 inclusion within the timescale or not. These decisions generated two new sets of  
1241 timescales containing 6791 and 6856 years within the top 540 m (Figure S1, black  
1242 dashed). While eliminating most of the discrepancies among the five interpreters, there  
1243 remained a difference of 65 years (1%) and 481 specific locations in the core where DW  
1244 and DF made different choices about the presence of an annual demarcation. DW made  
1245 one final round of choices after investigating the chemical stratigraphy surrounding each  
1246 of these years to reconcile the remaining differences into a single timescale containing  
1247 6826 years above 540 m (Figure S1, red). For comparison, roughly 6932 years would be  
1248 expected between 5 and 540 m based on volcanic synchronization, indicating that our  
1249 layer counting missed at least 106 years out 6932 (1.5%).  
1250



1251  
 1252 Figure S1: Offset between annual layer counting and SPICEcore-WAIS Divide tie points.  
 1253 Positive values on the y-axis indicate younger SPICEcore layer count ages relative to the  
 1254 synchronization with WAIS Divide (i.e. interpreters were missing years). Each blue line  
 1255 represents one of the 5 original independent sets of layer counts. The dashed black lines  
 1256 show the reconciled layer counted timescales after independent merging of the five  
 1257 original sets of picks by DW and DF. The red line indicates the final independent layer  
 1258 counted timescale. The green line shows the offset from SPICEcore-WAIS Divide tie  
 1259 points of automated layer counting using Straticounter (Winstrup et al. 2012) with the  
 1260 green shading inclusive of the 5<sup>th</sup> to 95<sup>th</sup> percentile ages. All of the layer counting efforts  
 1261 depicted were done independently of the stratigraphic tie points. All interpreters  
 1262 undercounted years, particularly during the interval from 228 to 275 m depth.

1263  
 1264

### ***S1.2 540-798 meters***

1265 Between 540 and 798 m, sampling resolution permitted further annual layer  
 1266 counting. One interpreter (DW) continued the counting to 798 m, below which point  
 1267 annual layers were not consistently detectable. DW counted 4597 layers between 540  
 1268 and 798 m, leading to an initial age of 11321 BP at the bottom of the annually dated  
 1269 section of the core.

### ***S1.3 Sections with Missing Data***

1270  
 1271 ***S1.3.1 Gaps and Damaged Core*** Within the top 798 m, where layer counting took place,  
 1272 there is a total of 2.74 m with missing data due to poor core quality or melter system  
 1273 errors. To fill these gaps in the timescale, we assigned an annual layer spacing equal to  
 1274 the average annual layer thickness of the 10 years above and below the gap. Layer  
 1275 thicknesses within the gap were rounded to make an integer number of equally spaced  
 1276 years. In total, 31 years were interpolated using this procedure.

1277 *S1.3.2 Dating the Top 5 meters* The SPICEcore chemistry dataset begins at 5.15 m below  
1278 the surface. We used chemistry from a hand-augered (HA) core drilled near the  
1279 SPICEcore drill site to date the uppermost firm. The HA core was recovered from the  
1280 surface to a depth of 9.86 m during the 2014/2015 field season; the same time as the  
1281 beginning of SPICEcore drilling. The short length allows us to date the HA core with  
1282 extra care using the following measurements: chloride, sulfate, sodium, magnesium,  
1283 liquid conductivity, particle counts (small channel),  $\text{Cl}^-/\text{Na}^+$  and  $\text{SO}_4^{2-}/\text{Na}^+$ . Layer  
1284 counting of the HA core indicates a date at 5.15 m between 1992 and 1993 (5.03=1993,  
1285 5.29=1992). The nearest volcanic tie point to the top of SPICEcore is at 10.58 m depth  
1286 with an age of -14 years before 1950 (1964 CE).

#### 1287 *S1.4 Validation with Straticounter*

1288 We performed a semi-independent check on our manual layer counting ability  
1289 using Straticounter, an automated layer counting software package described in  
1290 (Winstrup et al. 2012). This software has been used to aid in the dating of previous ice  
1291 cores in Greenland (Winstrup et al. 2012), Antarctica (Sigl et al. 2016), and Alaska  
1292 (Winski et al. 2017). We used the Straticounter program to identify annual layers within  
1293 the top 540 m of SPICEcore given sodium, magnesium, sulfate and microparticle data, as  
1294 well as the reconciled version of our layer counts. Results produce ages ranging from  
1295 6408 to 6615 years between 5-540 m, agreeing closely with 4 of the 5 interpreters, but  
1296 differing from the stratigraphically matched timescale by approximately 250-500 years  
1297 (Figure S1, green). Because of the scrutiny applied to the manual layer counting efforts,  
1298 and because the reconciled version of the hand-picked annual layer chronology is closer  
1299 to the stratigraphically coordinated timescale, we use the manual layer counts to  
1300 interpolate between tie points.

## 1301 **S2. Reconciling Layer Counts with Stratigraphic Ties**

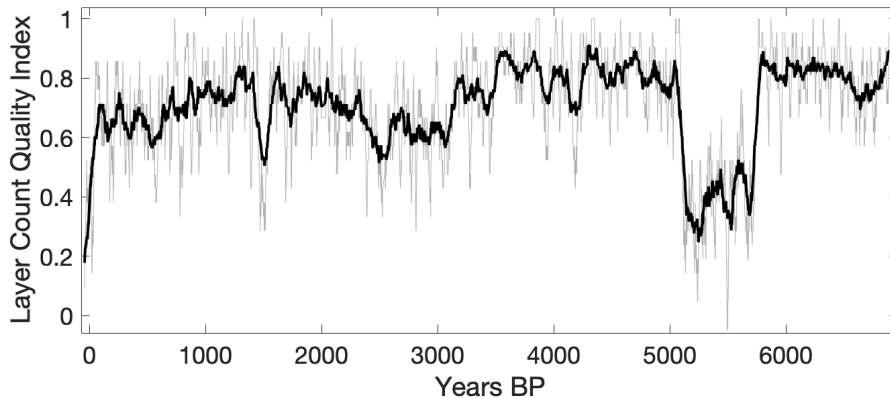
1302 To a depth of 798 m, 86 volcanic tie points to WAIS Divide were identified,  
1303 bracketing 85 depth intervals within which a known number of years must be present. To  
1304 make the layer-counted timescale consistent with these tie points, years were added or  
1305 subtracted, as necessary, within each interval such that the layer-counted timescale passes  
1306 through each tie point within +/- 1 year of its age, linking SPICEcore with the WAIS  
1307 Divide WD2014 chronology. In most intervals, very few years (1-5) needed to be added  
1308 or subtracted, although in certain sections layer counting consistently differed from the  
1309 WAIS-tied timescale. For instance, 105 years are missing between 228 and 275 m while  
1310 78 extra years were counted between 626 and 687 m. Because of the different counting  
1311 methods, procedures for adding and subtracting years differ above and below 540 m and  
1312 are described separately.

1313 Above 540 m, years were preferentially added or subtracted where DF and DW  
1314 disagreed in their final reconciliation (see Section S1.1). If an interval required the  
1315 addition or subtraction of a number of years that exceeded the number of disagreements  
1316 between DF and DW within the same interval, we first added years with 5 picks, then 4,  
1317 then 3, then 2, then 1 until we met the required number of years within each interval (the  
1318 opposite order applying to the subtraction of years). Between 540 and 798 m only one  
1319 interpreter (DW) picked layers, so positions where years were added or subtracted were

1320 selected manually. After adding or subtracting the appropriate number of years within  
1321 each interval, the layer-counted timescale passes within +/- 1 year of each stratigraphic  
1322 tie point. The Holocene layer-counted timescale is then merged with the Pleistocene  
1323 smoothest annual layer thickness interpolated timescale (Fudge et al. 2014) to form the  
1324 final SP19 timescale.  
1325

### 1326 S3. Layer Counting Performance

1327 Using multiple interpreters to develop the timescale provides the ability to assess  
1328 which areas contain better agreement among the different sets of picks. We assume that  
1329 our layer count chronology is more robust in regions where all 5 sets of picks agree (e.g.  
1330 Fig. 6A) than in regions with high discrepancy among picks (e.g. Fig. 6B). We create the  
1331 following index of layer count quality using the following rules: For picks where all  
1332 interpreters assigned a year within +/- 2 cm, we assign a value of 1. For picks where there  
1333 was disagreement among the five interpreters, but agreement between DW and DF while  
1334 reconciling, we assign a value of 0. For picks where there was disagreement between  
1335 DW and DF while reconciling, we assign a value of -1. By calculating smoothed values  
1336 of the layer count quality index over the top 540 m, patterns emerge showing areas of  
1337 higher and lower layer counting confidence (Fig. S2). Most notable is the section  
1338 between 412 and 456 m (5100 to 5700 BP) where analytical issues obscured robust  
1339 annual signals. Fortunately, this section is well constrained by volcanic events. The very  
1340 low accumulation values centered on 2400 BP are associated with another interval of  
1341 slightly lower certainty in our layer counting ability. This is partly due to a lack of  
1342 stratigraphic tie points, but the low accumulation here also caused all interpreters to  
1343 consistently undercount years (between 228 and 275 m) leading to greater potential  
1344 uncertainties.



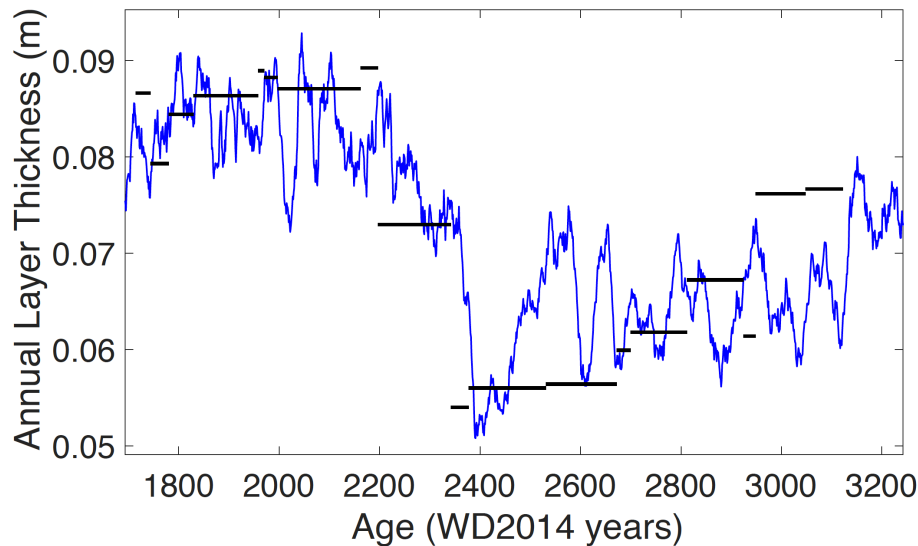
1345

1346 Figure S2: An index of layer counting quality over time. Higher values indicate greater  
1347 confidence in layer counting ability. The index reflects the level of agreement among the  
1348 five interpreters (see text). The 20-year (light gray) and 100-year (bold) running means  
1349 are shown.

1350

1351 **S4. Interval from 180 – 275 meters**

1352 We have identified only one tie point in the interval from 180m to 275m. Both  
1353 interpreters (TJF, DF) have spent considerable time examining this interval but have not  
1354 consistently identified the same events. The challenge of matching volcanic events in this  
1355 period has two primary causes: 1) a sharp change in accumulation rate and 2) numerous  
1356 small volcanic events. These two factors combine to make it difficult to distinguish  
1357 sequences of volcanic eruptions because the depth between events may be varying due to  
1358 the change in accumulation rather than a change in duration, and because there is no  
1359 distinct pattern to relative amplitudes of the events. One interpreter revisited this interval  
1360 to make another round of volcanic matches, which were made without any direct  
1361 information from the annual interpolation. These matches indicate a similar timescale to  
1362 the annual interpretation, which can be seen in Figure S3 of the average annual layer  
1363 thickness. However, the second interpreter did not find the same matches when revisiting  
1364 the interval and thus we exclude them from the underlying timescale.

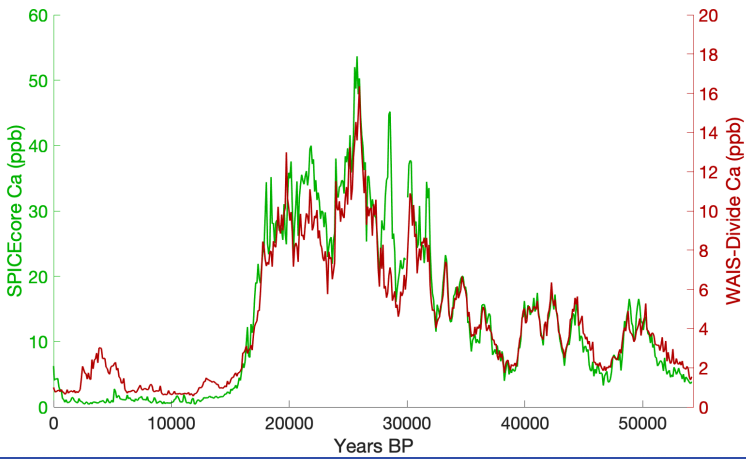


1365 Figure S3: Annual layer thickness comparison between the SP19 timescale (blue –  
1366 smoothed) and independent volcanic matches to WAIS-Divide (black). The volcanic  
1367 matches were made without reference to the annual layer counts yet show a very similar  
1368 pattern of annual layer thickness, further improving confidence in an accumulation  
1369 anomaly at this time.  
1370

1371 **S5. Time Series Comparisons Between WAIS-Divide and SPICEcore**

1372 Below, we show the calcium time series presented in Figure 12 of this manuscript  
1373 compared with an equivalent 100-year running median calcium record from WAIS-  
1374 Divide. Given the broad similarity in millennial-scale calcium variability among  
1375 Antarctic ice core records (e.g. Markle et al. 2018), there should be visible synchronicity  
1376 in the timing of events between the two records. Figure S5, shows that both the WAIS-

1377 [Divide and SPICEcore calcium records are closely matched \( \$r=0.96\$ ,  \$p<0.001\$ \) with a](#)  
1378 [maximum correlation with no offset between the two datasets. This provides further](#)  
1379 [support that none of the tie points selected to link the two ice cores are erroneous.](#)



1380  
1381 [Figure S5: Calcium concentrations in SPICEcore \(green\) compared with those in WAIS-](#)  
1382 [Divide \(red\). Both datasets are shown as 100-year medians. Shared events in calcium](#)  
1383 [concentration among the two cores are closely synchronized, supporting choices of tie](#)  
1384 [points between SP19 and WD2014. SPICEcore calcium data are preliminary.](#)

1385